J. Fluid Mech. (1982), *vol.* 119, *pp.* 55-89
Printed in Great Britain

Statistics of fine-scale velocity in turbulent plane and circular jets

By R. A. ANTONIA, B. R. SATYAPRAKASH

Department of Mechanical Engineering,
University of Newcastle, N.S.W. 2308, Australia

AND A. K. M. F. HUSSAIN

Department of Mechanical Engineering,
University of Houston, Texas 77004, U.S.A.

(Received 17 December 1980 and in revised form 19 October 1981)

Higher-order statistics of the streamwise velocity derivative have been measured on the centre-line of turbulent plane and circular jets. The instrumentation and sources of error are discussed to establish the accuracy of the data and convergence of statistics. The optimum setting for the low-pass filter cut-off was found to be 1·75 times the Kolmogorov frequency f_K, in contrast with the majority of previous investigations where it was set equal to f_K. The magnitude of the constant μ in Kolmogorov's revised hypothesis is obtained using statistics derived from the instantaneous velocity derivative or its squared value. The correlation and spectrum of fluctuations of the squared velocity derivative and the Reynolds-number variation of the skewness and flatness factors of the velocity derivative are consistent with $\mu \simeq 0{\cdot}2$, while the most popular value used is 0·5. Second-order moments of the locally averaged dissipation, assumed proportional to the squared streamwise velocity derivative, and breakdown coefficients also suggest a value of μ of about 0·2. Higher-order correlations and spectra of the dissipation are in closer agreement with the Novikov–Stewart or β-model than with Kolmogorov's lognormal model. Higher-order moments of locally averaged values of the dissipation rate are more closely represented by the lognormal than the β-model.

1. Introduction

A well-known feature of high-Reynolds-number turbulence is the spatial spottiness of its fine structure and hence of the dissipation rate ϵ of turbulent kinetic energy. Batchelor & Townsend (1949) measured probability-density functions of the streamwise velocity derivative $\partial u/\partial t$ ($\equiv \dot{u}$ hereinafter) and of the higher-order derivatives $\partial^2 u/\partial t^2$ and $\partial^3 u/\partial t^3$ downstream of a grid, and surmised that the energy associated with large wavenumbers is very unevenly distributed in space. They also identified 'isolated regions in which the large wavenumbers are activated, separated by regions of comparative quiescence'. Prompted by a remark by Landau (Landau & Lifschitz 1959), Kolmogorov (1962) and Obukhov (1962) modified Kolmogorov's earlier (1941) similarity hypotheses to include statistical properties of dissipation. The modification has led to a number of important consequences with regard to the Reynolds-number dependence of statistics of the fine-structure of turbulence (see Monin & Yaglom

1975). Specifically, Kolmogorov (1962) and Obukhov (1962) assumed that the probability density function of ϵ_r, the dissipation rate averaged over a local volume of characteristic dimension r, is lognormal. They also stated that it was natural to suppose that the variance σ^2 of $\ln \epsilon_r$ has the asymptotic behaviour (as $R_\lambda \to \infty$)

$$\sigma^2 = A + \mu' \ln (L/r) \quad (r \ll L), \tag{1}$$

where μ' is some universal constant, L is a length scale (the 'external' scale in Kolmogorov's paper) representative of energy-containing eddies, and A is a constant that may depend on the macrostructure of the flow. The assumed normality of $\ln \epsilon_r$, together with supposition (1), constituted, according to Kolmogorov (1962), a third hypothesis. In the rest of this paper we shall refer to these two assumptions as the lognormal, or LN, model. With these assumptions, the $-\frac{5}{3}$ exponent that appears in the $k_1^{-\frac{5}{3}}$ (k_1 is the one-dimensional wavenumber $2\pi n/U$, where n is the frequency and U the mean velocity) inertial-subrange form of the turbulent-energy spectrum (Obukhov 1941) is altered to $-\frac{5}{3} - \frac{1}{9}\mu'$. A basis for the two assumptions in LN was provided by Yaglom's (1966) and Gurvich & Yaglom's (1967) mathematical description of the cascade of sequential breakdown of turbulent eddies. Gurvich & Yaglom concluded that any non-negative quantity associated with the fine structure of turbulence has a probability-density function that is approximately lognormal with a variance similar to that given by (1).

In general, the average value in the inertial subrange $\eta \ll r \ll L$ (where $\eta = \nu^{\frac{3}{4}}/\bar{\epsilon}^{\frac{1}{4}}$) of the product $\epsilon(x)\,\epsilon(x+r)$ may be written as

$$\overline{\epsilon(x)\,\epsilon(x+r)} = D\bar{\epsilon}^2 (L/r)^\mu, \tag{2}$$

where μ is a universal constant and D is a constant which, like A, may depend on the macrostructure of the flow. The properties of the lognormal probability density function are such as to make (1) consistent with (2) when $\mu' \equiv \mu$ and $D \equiv e^A$ (e.g. Monin & Yaglom 1975, p. 618). With $\mu < 1$ Yaglom (1966), and Gurvich & Yaglom (1967) argued that the spectrum ϕ_ϵ of ϵ in the inertial subrange will be determined primarily by values of $\overline{\epsilon(x)\,\epsilon(x+r)}$ as given by (2), so that ϕ_ϵ will be of the form $k_1^{-1+\mu}$. This form of ϕ_ϵ was essentially obtained earlier by Novikov & Stewart (1964), who proposed a model, hereinafter referred to as NS, for dissipation fluctuations at high Reynolds number.

Mandelbrot (1974, 1976) introduced the concept of fractal dimension or measure of the extent to which the regions characterized by concentrations of dissipation fill space. He showed that the correction to the inertial-subrange form of the energy spectrum is less than or equal to $\frac{1}{3}\mu$ and that the correction $\frac{1}{9}\mu$ obtained from LN is only one of many possibilities. Kraichnan (1974) pointed out that, while the 1941 similarity theory is made implausible by the basic physics of vortex stretching, the 1962 modifications seem arbitrary, emphasizing that the idea of a self-similar cascade that produces systematically increasing intermittency with a decrease of scale size does not require the assumptions contained in Kolmogorov's third hypothesis. The idea of a multistage energy cascade, while simple and appealing, has been abandoned in physical models such as that proposed by Townsend (1951), who considered a random distribution of vortex sheets and lines to account for the spatial inhomogeneity of the motion. These physical models (also Corrsin 1962; Tennekes 1968; Saffman 1970) of the dissipation process all imply some statistical dependence between small

and large scales. It seems probable that these models may enjoy a resurgence of interest once the relating spatial geometry of these scales and the extent of interaction between these scales are better understood (Hussain 1980). Kraichnan (1974) commented that a central role for dissipation seemed arbitrary, since the dynamically relevant quantity is the local (nonlinear) rate of energy transfer and not the viscous dissipation. Frisch, Sulem & Nelkin (1978) introduced a model, called the β-model, of fine-structure intermittency. This model was described as dynamical in the sense that, in contrast with the LN and NS models, it deals with inertial-range quantities such as velocity amplitude and the locally defined energy-transfer variable. The β-model leads to a $\frac{1}{3}\mu$ correction to the $\frac{5}{3}$ exponent of the energy spectrum.

The exponent μ in the β and NS models is presumably the same as that in (2) (and therefore (1)), since these models predict a power-law form for the correlation $\overline{\epsilon(x)\,\epsilon(x+r)}$. Ideally, as noted by Kraichnan (1974), the value of μ should depend on the details of the nonlinear interaction embodied in the Navier–Stokes equation. Nelkin & Bell (1978) showed that all measurable scaling exponents for very-high-Reynolds-number turbulence can be expressed in terms of the exponent μ that describes the dissipation fluctuations.

Experiments have yielded a wide range of values for μ. Yaglom (1966) estimated a value of 0·4 for μ from measurements of the spectrum of ϵ. Values of μ in the range 0·17–0·8 reported in table 2 of Gibson & Masiello (1972) implied that the most probable value is 0·5. For $\mu \simeq 0{\cdot}5$ (a more reasonable estimate is suggested below), the inertial subrange-form of the modified energy spectrum is almost indistinguishable from the original $\frac{5}{3}$ behaviour. Measurements of spectra of u or $\partial u/\partial t$ would not therefore provide a meaningful test of the various models. A more stringent test of the various models would be provided by high-order statistics of ϵ, since differences between the models are expected to increase with increasing order of statistics. While the LN, NS (also Novikov 1965) and β-models are all consistent with (2), the generalization of (2) using LN (Gurvich & Yaglom 1967; Monin & Yaglom 1975, p. 620) is

$$\overline{\epsilon^m(x)\,\epsilon^n(x+r)} \sim (L/r)^{\mu mn} \tag{3}$$

for $m, n \geqslant 1$. The NS and β-models yield

$$\overline{\epsilon^m(x)\,\epsilon^n(x+r)} \sim (L/r)^{(m+n-1)\mu}. \tag{4}$$

Since the dependence of the exponent on m (usually chosen equal to n) is quadratic in (3) and linear in (4), the differences between predictions (3) and (4) increase as m and n increases. The measured correlation $\overline{\epsilon^m(x)\,\epsilon^n(x+r)}$ (for $m = n = 1$, 1·5 and 2) by Gagne & Hopfinger (1979) showed that the dependence on the exponent in the power law was linear, but the decrease with respect to r was not as rapid as that indicated by (3).

One of the difficulties in comparing experimental results with (3) or (4) appears to be the questionable universality of μ. For example, Frenkiel & Klebanoff (1975) concluded that their measurements of high-order moments of $\dot{u}$ in grid turbulence and in a turbulent boundary layer 'correlated in a form related to lognormality of the probability of dissipation but did not conform to the requirement imposed by log-normality of a constant μ'. Frenkiel & Klebanoff (see also Frenkiel, Klebanoff & Huang 1979) also concluded that the non-constancy of μ is not necessarily due to an insufficiently large turbulent Reynolds number R_λ (defined as $(\overline{u^2})^{\frac{1}{2}}\lambda/\nu$, where λ is the

Taylor microscale $U(\overline{u^2})^{\frac{1}{2}}/(\overline{\dot{u}^2})^{\frac{1}{2}}$ or to the fact that the measurements were made in different flows. Measurements of normalized even-order moments $\overline{\dot{u}^{2n}}/(\overline{\dot{u}^2})^n$ ($n = 2$–7) by these authors indicated that μ decreased from about 0·2 to about 0·1 as n increased. A value of $\mu \simeq 0{\cdot}2$ would be a good approximation for the flatness-factor ($n = 2$) distribution for a wide range of values of R_λ. Van Atta & Antonia (1980) found that $\mu \simeq 0{\cdot}25$ yielded good agreement between the prediction of their analysis and the experimental values of the skewness $S\,(\equiv \overline{\dot{u}^3}/(\overline{\dot{u}^2})^{\frac{3}{2}})$ and flatness factor $F\,(\equiv \overline{\dot{u}^4}/(\overline{\dot{u}^2})^2)$ of $\dot{u}$ for $R_\lambda > 200$.

Although measurements of high-order moments (see for example the probability density functions of $\dot{u}$ shown in figure 3.13 of Wyngaard 1973) and high-order spectra (e.g. Champagne 1978) of $\dot{u}$ indicate a dependence on R_λ that is qualitatively consistent with predictions by both statistical and physical models for the fine-structure intermittency, quantitative agreement between experiment and predictions is not entirely satisfactory. Tennekes & Wyngaard (1972) and Frenkiel & Klebanoff (1975) have considered the measurement difficulties that exist when high-order moments of $\dot{u}$ are sought. While improvements in the models may be necessary before satisfactory agreement with measurements can be achieved, it seems equally important that a reliable data base is first established before a meaningful comparison between predictions and measurements can be made. In the present laboratory experiments, high-order moments of $\dot{u}$ and high-order spectra of $\dot{u}$ are measured at different streamwise locations on the centre-line of a circular jet and on the plane of symmetry of a plane jet. All locations are in the self-preserving region of these flows. Attention is given to the setting of the cut-off filter prior to digitization of the data. Data-processing requirements, such as the integration time necessary to ensure adequate accuracy of the data, are also considered. Values of μ obtained using a number of different statistics of $\dot{u}$ are discussed with a view to clarifying the present confusion with regard to the determination of μ. The measurements have been obtained over a reasonably wide range of R_λ, approximately 300–1000, to enable comparison with the Reynolds-number dependence suggested by different models. Measured higher-order correlations and spectra of $\dot{u}^2$ are compared with predictions from these models.

2. Experimental facilities and conditions

A brief description only of the plane jet facility is given here as details may be found in Hussain & Clark (1977). The jet nozzle is a 1·4 m long two-dimensional contraction from the 1·4 m square settling chamber to the 3·18 cm × 140 cm vertical slit exit. The jet exists between two 3 m long horizontal bounding plates and normal to a nozzle end plate (2 m wide) with rounded leading edges to ensure a separation-free, entrainment-induced boundary layer on the plate. Since the work reported by Hussain & Clark, the AC motor driving the jet has been replaced by a variable-speed DC motor, to enable continuous variation of the jet speed. The jet exit velocity U_j is 9·64 m/s, which corresponds to a Reynolds number $R_d\,(\equiv U_j d/\nu) = 2{\cdot}04 \times 10^4$.

The circular jets used for this study are of two different diameters ($d = 2{\cdot}54$, 18 cm). The 2·54 cm diameter nozzle (Batchelor–Shaw profile) is used with the jet facility described in Hussain & Zedan (1978). The nozzle is made from laminated wood blocks so that the jet emerges through a 30 cm diameter end-plate. Air from a six-blade blower driven by a DC motor passes through a silencer section, a 10° diffuser fitted

with screens, before entering the first settling chamber through a honeycomb (5·08 cm deep hexagonal cells, 3·2 mm cell size). Downstream of the settling chamber is an axisymmetric contraction, a 6° diffuser, a number of screens (11·4 mesh/cm) and the 2·54 cm diameter nozzle.

The larger circular jet-flow facility has been described by Husain & Hussain (1979), except that a new 18 cm diameter fibre-glass nozzle was used for the present study. The nozzle is attached to the end of a 5 m long settling chamber of 76 cm diameter, containing ten screens of 9·5 mesh/cm and 47 % solidity. The nozzle is 1·0 m long and has a contour whose radius at any streamwise location is the mean of the radii corresponding to Batchelor–Shaw and cubic-equation contours (see Hussain & Ramjee 1976). This nozzle does not have an end-plate, so that entrained air merges essentially parallel to the stream at the lip.

The plane and circular jet facilities are located in a large laboratory (30 m × 15 m × 3·5 m) with controlled temperature and humidity. All the three facilities discharge into a sufficiently large empty space so that ambient turbulence is not likely to be significant. These facilities are operated one at a time. They are driven by DC motors controlled by full-wave rectifiers (built in-house) so that the blower speed can be set at any desired value as well as held constant over a long time. The centre-line longitudinal fluctuation intensity in the exit plane of all the jets is about 0·28 %. The exit boundary-layer mean profile in each case agrees with the Blasius profile, and the peak fluctuation intensity in the boundary layer, unavoidable owing to settling-chamber cavity resonance (Hussain & Clark 1977), is less than 1·2 %. All three facilities are built of separate modules connected together by flexible rubber sheets, and the blower–motor assemblies are isolated from the laboratory floor; thus the jet flows are free from any perceptible vibration of the nozzle, tunnel or laboratory floor. Experimental values of R_d for $d = 2{\cdot}54$, 18 cm are respectively $5{\cdot}56 \times 10^4$ and $4{\cdot}71 \times 10^5$.

The velocity fluctuation is measured with a 2·5 μm diameter Wollaston (Pt–10 % Rh) hot wire (length approximately 0·52 mm) operated by a DISA 55M10 constant-temperature anemometer at an overheat ratio of 0·8. The frequency response of the wire and anemometer, determined by the square-wave technique, extends up to about 100 kHz for the present experimental conditions. The output voltage from the anemometer is AC coupled via a DISA 55D26 signal conditioner (DC to 100 kHz) to a Krohn-Hite model 3341 low-pass filter (-3 dB cut-off frequency f_{c1} with 48 dB/octave roll-off) before differentiation using an operational amplifier in the differentiating mode (no departure from linearity could be discerned up to 100 kHz). The differentiator was designed for a gain of unity at 7 kHz. The output voltage from the differentiator was passed through another Krohn-Hite 3341 low-pass filter (-3 dB cut-off frequency $f_{c2} (= f_{c1})$ and of identical phase characteristics to the filter used prior to differentiation). Signals at the outputs from the two filters were fed to a DISA 55D35 TRUE RMS meter to obtain r.m.s. values of u and $\dot{u}$. These signals were also digitized using a 12-bit resolution A–D converter, prior to subsequent data processing by PDP11/20 and 11/34 digital computers. The effect of any possible temperature contamination of the hot wire on the statistics of $\dot{u}$ was negligible, primarily because the mean temperature at all measurement stations was very close to the controlled ambient temperature of the laboratory.

3. Experimental procedure and accuracy of data

Difficulties in obtaining reliable measurements of small-scale turbulence have already been discussed by previous investigators. Tennekes & Wyngaard (1972) discussed signal-to-noise and integration-time limitations that make measurements of moments higher than the fourth extremely difficult for large-R_λ turbulence, such as that encountered in the atmospheric surface layer. Frenkiel & Klebanoff (1975) obtained moments up to order 14 of u, in grid turbulence and in a boundary layer. In view of the severe requirements imposed on the measurements, effects such as averaging intervals and convergent tails of the probability density functions were given special attention. Champagne (1978) obtained new data on the fine structure of the velocity field in both the atmospheric surface layer and various laboratory flows, and examined these data for evidence of universal behaviour and local isotropy. In his section on interpretation of data, he states that data obtained by previous investigators were eliminated from consideration on the basis of a number of points:

(i) the length of the sensors is much greater than the Kolmogorov microscale $\eta\,(\equiv \nu^{\frac{3}{4}}/\bar{\epsilon}^{\frac{1}{4}})$;

(ii) low-pass filter setting equal to or less than the Kolmogorov frequency f_K $(\equiv U/2\pi\eta)$;

(iii) inadequate averaging time, resulting in excessive scatter.

The above points, and two further considerations, are discussed below in connection with the present measurements.

3.1. *Spatial resolution*

The spatial resolution of the sensor is clearly important to the study of the fine structure. The diameter $d_w\,(= 2{\cdot}5\ \mu\text{m})$ and length $l_w\,(\simeq 0{\cdot}52$ mm) of the hot wire were chosen so that the ratio l_w/η was as small as practicable, while l_w/d_w was sufficiently large. For $x/D > 60$, l_w/η decreased from about 2·5 to 1·0. For the data considered by Champagne (1978), l_w/η was in the range 0·52–2·94. In Gagne & Hopfinger's (1979) experiment, $l_w/\eta \leqslant 2$ and $l_w/d_w \simeq 350$. This was achieved by using a hot wire of 1 μm diameter, operated by a specially built constant-current anemometer. In the present experiment $l_w/d_w \simeq 200$, which is similar to that used in Champagne's (1978) investigation. Champagne, Sleicher & Wehrmann (1967) found that for a wire with $l_w/d_w = 200$ and at an overheat ratio of 0·8, the end conduction loss represents about 8 % of the convective loss. For a tungsten wire with $l_w/d_w \simeq 200$ and an overheat ratio of 1·0, Bradshaw (1971) estimates that the end conduction loss is about 15 % of the convective loss. For sufficiently large l_w/d_w, hot-wire length corrections at the high-frequency end of ϕ_u (ϕ denotes spectral density) arise because the instantaneous wavenumber vector is not normal to the wire and because of inherent attenuation at extremely large wavenumbers. Both effects worsen with increasing l_w/η (Wyngaard 1968). Wyngaard's calculations show that for a wire of length 3η, ϕ_u is underestimated by about 6 % at $k_1 l_w = 1$. It should be further noted that Wyngaard's calculations are based on a theoretical form of the spectrum that precludes any dependence on R_λ, at variance with the experimental observation of Champagne (1978). Once the experimental variation, at relatively large $k_1\eta$, of $\phi_{\dot{u}}$ with R_λ is established, Wyngaard's correction procedure could perhaps be modified so that the hot-wire length

correction also depends on R_λ. Another approach for applying wire-length corrections is to use a reference spectrum measured by an ideal ($l_w/\eta \leqslant 1$) sensor. Such an approach was used by Schedvin, Stegen & Gibson (1974). To reconcile their direct dissipation measurements made behind a large grid with decay-law values, these authors used an iterative wire-length correction procedure based on a comparison with a reference spectrum (measurements in a cylinder wake with $R_\lambda = 258$) for which $\eta/l_w = 0{\cdot}75$. It was suggested, using the results of the empirical wire-length correction, that Wyngaard's (1968) theoretical correction, based on Pao's (1965) spectrum, seriously underestimated the actual correction. In view of the experimentally observed (Champagne 1978) variation of the high-wavenumber part of the spectrum with R_λ, the correctional procedure of Schedvin *et al.* (1974) does not seem practical, since the 'correct' spectra at any arbitrary R_λ are not known *a priori*. No length correction was used in the present investigation, as such correction will fall within the scatter of the $\phi_{\dot{u}}$ data.

3.2. *Cut-off frequency*

The cut-off frequency settings f_{c1} and f_{c2} for the two Krohn-Hite filters (§ 2) were determined at each measurement location. f_{c1} was first, somewhat arbitrarily, set equal to a relatively high frequency, typically twice the upper limit of the spectral content of $\dot{u}$. The spectral density $\phi_{\dot{u}}$ obtained using a real-time spectrum analyser (SD335), was displayed on the built-in oscilloscope of the analyser to determine f_{c1} visually. The frequency f_{min} of the lowest point on the spectrum, which occurs before the increase due to noise, can be easily determined. Since there is some noise contribution to the spectrum for $f < f_{min}$, the correct setting for the filter cut-off should be less than f_{min}. From the spectral display the frequency f_c ($< f_{min}$) at which $\phi_{\dot{u}}$ exceeds by 2 dB that at f_{min} was accurately determined using the scope cursor. Both f_{c1} and f_{c2} were then set at this value. Although the choice of 2 dB is somewhat arbitrary, it was found that, at most measurement locations, the value of f_{c1} (or f_{c2}) was approximately $2f_K$. For the present experimental conditions, $\phi_{\dot{u}}(f_{c1})$ was typically 30 dB below the maximum value of $\phi_{\dot{u}}$, which occurs at approximately $\frac{1}{10}f_K$.

3.3. *Integration time*

The integration time required for a moment to reach a stable value increases as the order of moment increases because progressively higher moments are dominated by the extreme and rarer excursions. An estimate of this time can be obtained from the relation (Tennekes & Lumley 1972, p. 212)

$$\omega^2 = 2\left(\frac{\overline{\dot{u}^{2n}}}{(\overline{\dot{u}^n})^2} - 1\right)\frac{I_n}{T}, \tag{5}$$

where ω^2 is the mean-square relative error of $\overline{\dot{u}^n}$, T is the total record duration and I_n is the integral time scale of ξ_n ($\equiv \dot{u}^n - \overline{\dot{u}^n}$), defined as

$$I_n = \frac{1}{\overline{\xi_n^2}}\int_0^\infty \overline{\xi_n(t)\,\xi_n(t+\tau)}\,d\tau. \tag{6}$$

The autocorrelation was obtained by computing the inverse Fourier transform of the spectrum ξ_n. The integral time scale I_1 of the velocity derivative is zero (e.g. Tennekes & Lumley 1972, p. 216). To evaluate I_n ($n \geqslant 2$), the time corresponding to the first zero-crossing of the autocorrelation was (arbitrarily) taken, instead of ∞, as the upper

limit of integration of (6). For $n = 3$, the absolute value of $\dot{u}^3$ was considered, since the integral time scale of any odd-order moment of $\dot{u}$ should be zero and (5) is consequently invalid when n is odd. Values of I_n ($n \geqslant 2$) fall within the following ranges: $I_2 U/\eta = 10 \pm 2$, $I_3 U/\eta = 4{\cdot}5 \pm 0{\cdot}3$, and $I_4 U/\eta = 2{\cdot}5 \pm 0{\cdot}5$. The average value of $I_2 U/\eta$ is in reasonable agreement with the estimate inferred by Tennekes & Wyngaard (1972) from results of Wyngaard & Pao (1972) and Friehe, Van Atta & Gibson (1971). It is, however, a factor of 2 smaller than the estimate of Champagne, Pao & Wygnanski (1976). Tennekes & Wyngaard (1972) concluded that I_4 and I_6 were also of the order of $10\eta/U$ on the basis of spectra obtained by Friehe *et al.* (1971). The present data do not support this conclusion, the discrepancy perhaps being due to the different methods of evaluating I_n (Tennekes & Wyngaard extrapolated the spectrum of $\dot{u}^n$ to $k_1 = 0$ to obtain I_n). The reduction in I_n as n increases is, as noted by Sreenivasan, Chambers & Antonia (1978), of some importance in assessing the accuracy of high-order moments. It is of interest to compare the present values of I_n with those obtained by Sreenivasan *et al.* (1978), who considered nearly Gaussian velocity and temperature fluctuations in both the laboratory and atmosphere. These authors found that I_n/I_1 did not decrease monotonically with n (the present values of I_2, I_3 and I_4 are consistent with this trend), but suggested that a useful first approximation for this ratio was given by

$$I_n/I_1 = 0{\cdot}82 - 0{\cdot}07n.$$

These values of I_n/I_1, at least for $n = 2$ and $n = 3$, are in reasonable agreement with those calculated by Alekseev (quoted by Lumley 1970), who assumed a Gaussian process and an exponential form for the autocorrelation function. The ratio I_4/I_2 is then approximately 0·79, which is considerably larger than the present average value of 0·25 for this ratio. While the difference is perhaps associated with the non-Gaussian character of $\dot{u}$, it should be recalled that values of I_n/I_1 obtained by Sreenivasan *et al.* (1978) for (non-Gaussian) products of velocity fluctuations are only slightly smaller than those obtained for the approximately Gaussian individual velocity fluctuations. Using the present values of I_n, record durations required to obtain moments with 5 % error ($\omega^2 = 25 \times 10^{-4}$) were determined. The square brackets in figure 1 indicate these durations for the variance and flatness factors of $\dot{u}$. The non-dimensional parameter TU/L_0 (where L_0 is the transverse distance from the axis to the location where the velocity is $\frac{1}{2}U$) for skewness is found to lie in a range 2×10^3 to $3{\cdot}5 \times 10^3$. The duration required for 5 % error of the variance is only 3–10 % of the experimental record duration (approximately 150 s for all data considered here) whereas for the skewness and flatness factors, T represented respectively 115 ($\pm$ 20) % and 65 ($\pm$ 15) % of the experimental record duration. Gagne & Hopfinger (1979) assumed a value of $I_4 U/\eta \simeq 10$, and estimated that, for their duct-flow data ($R_\lambda = 310$), a record duration of 32 s was sufficient to provide $\overline{\dot{u}^4}$ to better than 2 % error. While their estimate may be thought to be conservative since I_4 is likely to have been overestimated, their value of $\overline{\dot{u}^8}/(\overline{\dot{u}^4})^2$ is 160, while the present data, for a comparable R_λ ($\simeq 388$), indicates a value of $\overline{\dot{u}^8}/(\overline{\dot{u}^4})^2$ of about 372. There seems little doubt that T, as given by (5), would increase as R_λ increases, owing to the excursions in $\dot{u}$ being larger and rarer at larger R_λ.

The variation of $\overline{\dot{u}^{2n}}/(\overline{\dot{u}^2})^n$ with R_λ would need to be established accurately before (5) can be used for reliable predictions of T or ω^2. Figures 2 and 3 show running averages of $\dot{u}^n$ for the small- and large-diameter circular jets respectively. As a criterion for convergence, the time required for each moment to converge to within 5 % of its final

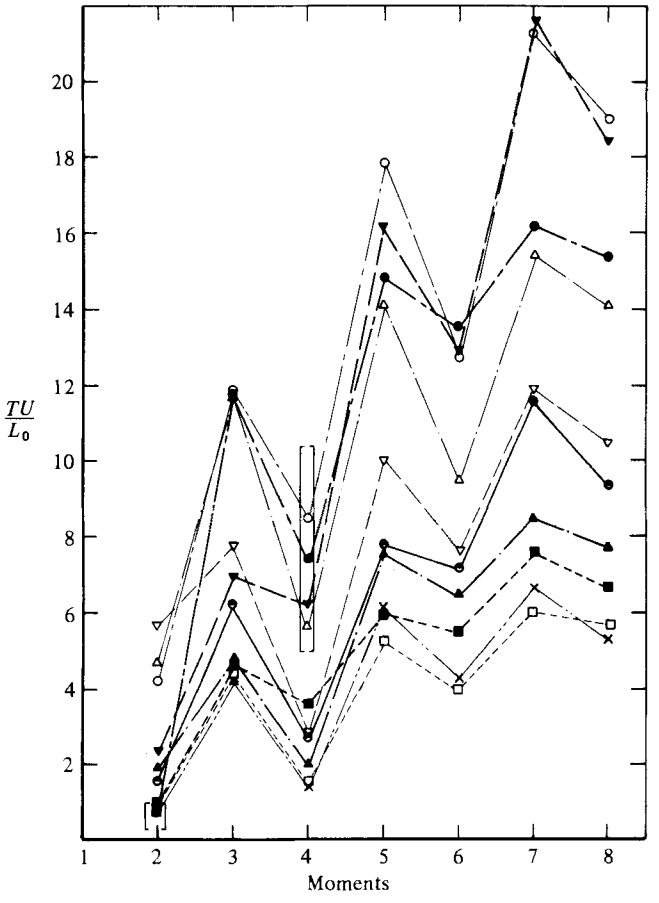

FIGURE 1. Record duration T required to achieve an accuracy of 5% for moments of order n of $\dot{u}$. Square brackets indicate values obtained using (5). Symbols refer to convergence times obtained from running means. Circular jet, d = 18 cm: ×, x/d = 50. Circular jet, d = 2·54 cm: ○, x/d = 70; △, 80; ▽, 90; □, 120. Plane jet: ▼, x/d = 60; ●, 80; ◓, 100; ▲, 120; ■, 140.

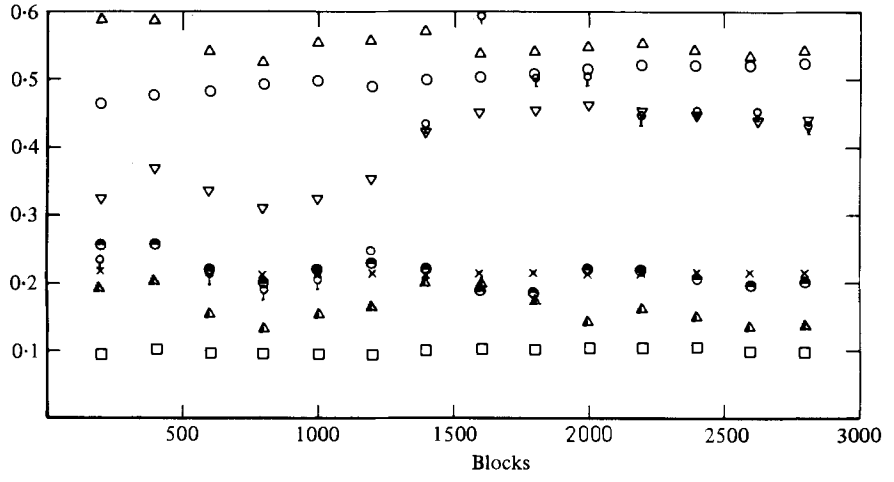

FIGURE 2. Running averages for moments, up to the 8th order, of $\dot{u}$ for the 2·54 cm circular jet (x/d = 90) as a function of record duration. 1000 blocks correspond to a duration of 53·78 s. ×, mean; ○, r.m.s.; △, $-\overline{\dot{u}^3}/(\overline{\dot{u}^2})^{\frac{3}{2}}$; □, $(\overline{\dot{u}^4}/(\overline{\dot{u}^2})^2) \times 10^{-2}$; ◓, $-(\overline{\dot{u}^5}/(\overline{\dot{u}^2})^{\frac{5}{2}}) \times 10^{-2}$; ▽, $(\overline{\dot{u}^6}/(\overline{\dot{u}^2})^3) \times 10^{-3}$; △, $-(\overline{\dot{u}^7}/(\overline{\dot{u}^2})^{\frac{7}{2}}) \times 10^{-4}$; ♀, $(\overline{\dot{u}^8}/(\overline{\dot{u}^2})^4) \times 10^{-5}$.

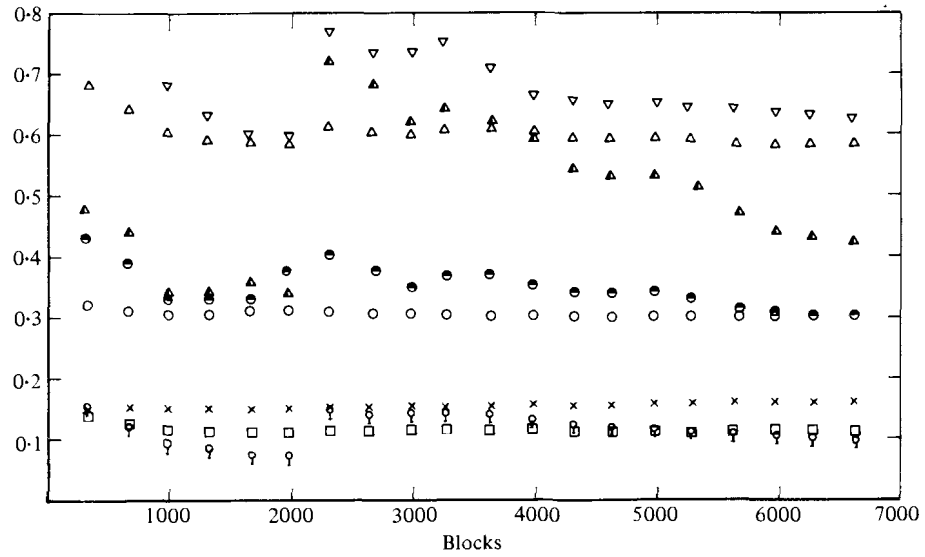

FIGURE 3. Running averages for moments, up to the 8th order, of $\dot{u}$ for the 18 cm diameter jet (x/d = 50) as a function of record duration. 1000 blocks correspond to a duration of 22·68 s. Symbols are as in figure 2, except that, for ♀, the multiplying factor is now 10^{-6}.

value was determined for the data. Convergence times obtained in this fashion are shown in figure 1. Similar symbols, appropriate to a particular flow but for different values of n, have, for clarity, been joined by straight lines. As in the case of convergence times for temperature structure functions (Antonia & Van Atta 1978), the data in figure 1 indicate that even-order moments converge more rapidly than odd-order moments. It is also clear that the time estimated from (5) for $|\dot{u}^3|$ is significantly larger than the convergence times obtained from the running averages of $\dot{u}^3$.† For $n = 2$, the measured convergence times for the small circular jet are considerably larger than estimates from (5), but the two methods seem to agree for the higher-R_λ data. It is difficult to make a meaningful comparison of estimates by the two methods, since a precise correspondence between the convergence time defined here and the time derived from (5) has not been established. On the basis of present convergence-time estimates, it may be asserted that the present record duration is adequate to ensure stability of moments of $\dot{u}^n$. It is also interesting to note that the rate of increase of the convergence times for the two separate curves in figure 1 is somewhat analogous to that exhibited by the curves of Antonia & Van Atta (1978), although the latter curves were obtained for structure-function data in the inertial subrange. Figures 2 and 3 indicate that running moments have generally large values at the start of the record, but the decrease towards a final value with increasing record time is monotonic only in the case of the first two or three moments. Running values of the mean, r.m.s., skewness and flatness factors of $\dot{u}$ are generally well-behaved with record duration, but higher-order moments do sometimes exhibit unexpected jumps. This is clearly the case in figure 3, where moments of order 5 to 8 all show a sudden increase at approximately one third ($\simeq$ 2000 blocks) of the record duration, and decrease only slowly to a final value at the end of the record. Note that the finality of this value is perhaps questionable with respect to the large circular jet ($R_\lambda \simeq 966$).

† Running averages of $|\dot{u}^3|$ were not obtained.

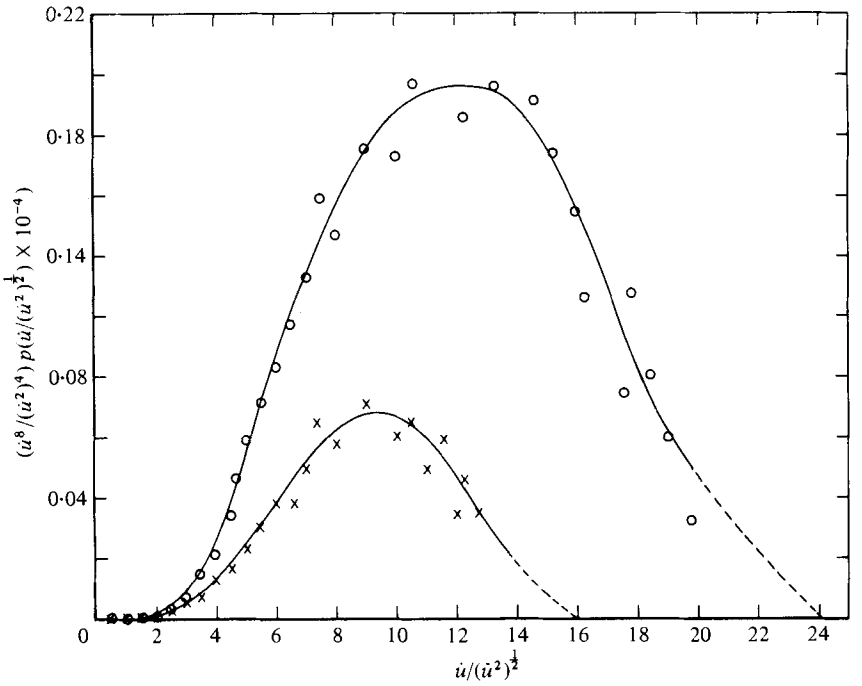

FIGURE 4. Normalized eighth-order moment integrand distributions for $p(\dot{u}/(\overline{\dot{u}^2})^{\frac{1}{2}})$. Plane-jet data ($x/d = 100$): ○, negative $\dot{u}$; ×, positive $\dot{u}$.

3.4. *Convergence of p.d.f.*

The measurement of higher-order moments requires that particular attention be given to the closure of the tails of probability-density functions. The average value of $\dot{u}^n$ can be written as

$$\overline{\dot{u}^n} = \int \dot{u}^n p(\dot{u})\, d\dot{u},$$

where the probability-density function $p(\dot{u})$ of $\dot{u}$ is such that

$$\int p(\dot{u})\, d\dot{u} = 1.$$

Values of $\overline{\dot{u}^n}$ were computed directly from the digital record and also using the probability-density function. The magnitude of the integrand $\dot{u}^4 p(\dot{u})$ decreased towards zero at large values of $|\dot{u}|$. For $R_\lambda = 580$, the integrand was negligible at $\dot{u} \simeq -12(\overline{\dot{u}^2})^{\frac{1}{2}}$ (for $n = 4$), whereas at $R_\lambda = 966$, for $n = 4$, the integrand was almost zero at

$$\dot{u} \simeq -17(\overline{\dot{u}^2})^{\frac{1}{2}}.$$

Closure of the tails of $p(\dot{u})$ was reasonable even at $n = 8$, the largest power considered here, thus indicating that the dynamic range of the signal-processing equipment was satisfactory. The curve fits (visual) through positive and negative values of

$$(\dot{u}^8/(\overline{\dot{u}^2})^4)\, p(\dot{u}/(\overline{\dot{u}^2})^{\frac{1}{2}})$$

shown in figure 4, yield a value of $\overline{\dot{u}^8}/(\overline{\dot{u}^2})^4$ that is within 15 % of the value obtained from the digital record.

3.5. *Effect of Taylor's hypothesis*

In Champagne's (1978) investigation, corrections due to the effect of a fluctuating convection velocity on Taylor's hypothesis ($\partial/\partial x \equiv -U^{-1}\partial/\partial t$) were applied to several statistics of $\dot{u}$. In particular, 'correct' values of the mean dissipation and of the skewness of $\dot{u}$ were evaluated, and the high-wavenumber end of the spectrum was corrected using a model developed by Lumley (1965).† Heskestad (1965) and Lumley have shown that the use of Taylor's hypothesis overestimates $\bar{\epsilon}$ in high-intensity turbulence, since

$$\overline{\dot{u}^2} = U^2\overline{\left(\frac{\partial u}{\partial x}\right)^2}\left(1+\frac{\overline{u^2}}{U^2}+2\frac{\overline{v^2}+\overline{w^2}}{U^2}\right). \tag{7}$$

Application of this formula to the present measurement indicates that $\overline{(\partial u/\partial x)^2}$ is overestimated by about 22 % and 32 % for the plane and circular jets respectively. Antonia, Phan-Thien & Chambers (1980) have discussed the assumptions underlying (7), and concluded that the application of this correction may not be fully justifiable. They also suggested that, since little is known about $\partial u/\partial x$, statistics of $\partial u/\partial x$ formed by dividing $\dot{u}$ by $U+u$ may be more attractive from an experimental point of view than those derived by applying (7). In particular, they obtained

$$\overline{\dot{u}^2} \simeq U^2\overline{\left(\frac{\partial u}{\partial x}\right)^2}\left(1+3\frac{\overline{u^2}}{U^2}+5\frac{\overline{u^4}}{U^4}\right)^{-1}, \tag{8}$$

with the assumption that $\dot{u}$ and $U+u$ are independent. The correction suggested by (8) is in the opposite direction to that indicated by (7). Application of (8) leads to $\overline{(\partial u/\partial x)^2}$ being underestimated by about 16 % and 20 % for the plane and circular jets respectively. Antonia, Phan-Thien & Chambers (1980) noted that further work was required on the independence between small and large scales of motion before a choice could be made between (7) and (8). Pending such an investigation, no corrections have been applied in the present work to either second- or higher-order moments of $\dot{u}$.

4. Results and discussion

4.1. *Effect of low-pass filter cut-off*

The effect of varying the low-pass filter cut-off f_c on the flatness factor and skewness of $\dot{u}$ for the plane jet is shown in figure 5. It is clear that the magnitudes of the flatness factor F and skewness S of $\dot{u}$ first increase with f_c before a maximum is reached at approximately $1{\cdot}75f_K$. This maximum is not pronounced in that there is no significant variation in S or F in the range $1{\cdot}5 < f_c/f_K < 2$. No measurements were obtained for f_c greater than about $2{\cdot}5f_K$, but it is expected that the effect of noise will become more pronounced at large values of f_c and that $|S|$ and F will consequently decrease. A qualitatively similar behaviour of F as a function of f_c was observed by Kuo & Corrsin (1971), but the frequency at which the plateau was first reached was approximately equal to f_K, at least for relatively small values of R_λ (< 350). At $R_\lambda \simeq 850$ (axis of a 15·2 cm diameter jet), the variation of F with f_c suggests that a maximum

† Chock (1978) extended Lumley's model to estimate the effect of a fluctuating convection velocity on the eddy-convection velocity for the high-frequency end of velocity and scalar spectra.

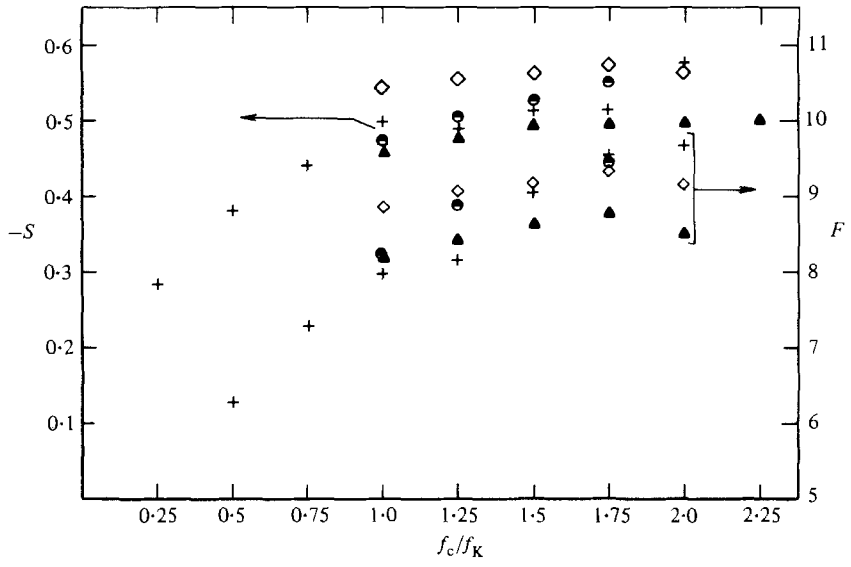

FIGURE 5. Skewness and flatness factors of $\dot{u}$ as functions of cut-off frequency f_c. Plane jet: ◓, $x/d = 80$; +, 100; ◇, 120; ▲, 140.

will only be reached at $f_c > 1{\cdot}5f_K$, in agreement with the present experimental trend. Kuo & Corrsin also considered the flatness factor of the second derivative $\partial^2 u/\partial t^2$ as a function of f_c. These data seem to indicate, almost independently of R_λ, that the maximum is reached near $1{\cdot}75f_K$. The data of figure 5, and other data obtained for S and F in the two circular jets, indicate that $f_c = 1{\cdot}75f_K$ may be more appropriate than $f_c = f_K$, a cut-off setting that has been used in several previous investigations. The setting $f_c = 1{\cdot}75f_K$ does not appear to depend on R_λ, at least for the present relatively small R_λ range. All results presented in this paper are obtained using this f_c setting and a sampling frequency of $2f_c$. Some support for this setting is provided by Gagne & Hopfinger (1979) and Gagne, Hopfinger & Marechal (1979), who found that F shows a maximum at $f_c \simeq 2f_K$ and recommend that the sampling frequency should be greater or equal to $4f_K$. Frenkiel & Klebanoff (1975) initially adopted the recommendation by Kuo & Corrsin (1971) that $f_c \simeq f_K$, but more recently Frenkiel *et al.* (1979) verified that $f_c \simeq f_K$ is the appropriate setting, at variance with the present result. Moments, up to order 14, of $\dot{u}$ obtained for grid turbulence in water indicated that the maximum occurs at $f_c \simeq f_K$ when $R_\lambda \simeq 123$. At a slightly higher value of R_λ (= 202), the maximum occurred at $f_c \simeq 0{\cdot}63f_K$. While the results of Frenkiel *et al.* (1979), when compared with the present results, appear to suggest that the particular setting of f_c may depend on R_λ, this suggestion is not really supported by the measurements of Kuo & Corrsin (1971) and Gagne & Hopfinger (1979), which were obtained at values of R_λ only marginally larger than those considered by Frenkiel *et al.* (1979). The variation (not shown here) of the fifth- and sixth-order moments of $\dot{u}$ with f_c/f_K is such that $f_c \simeq 1{\cdot}75f_K$ remains an appropriate choice for the filter setting. With reference values taken for $f_c \simeq 1{\cdot}75f_K$, the use of $f_c = f_K$ would, on average, underestimate both S and F by about 10 %. In the case of the normalized fifth- and sixth-order moments of $\dot{u}$, the errors are approximately 27 % and 23 % respectively.

The variation of $\overline{\dot{u}^n}/(\overline{\dot{u}^2})^{\frac{1}{2}n}$ along the axis of both plane (figure 6) and circular

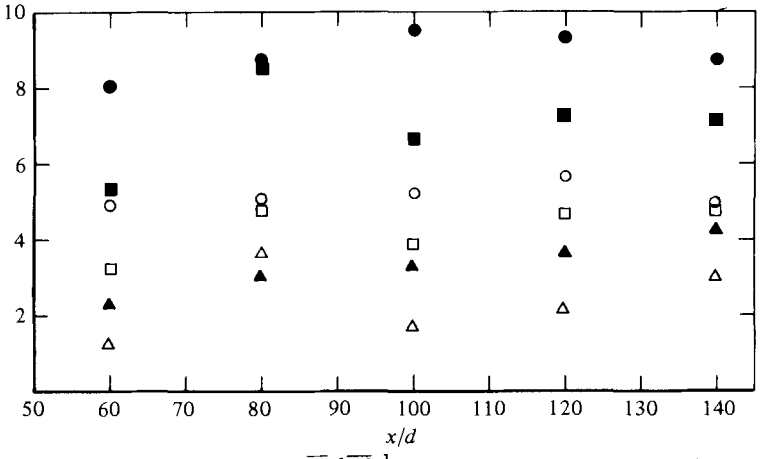

FIGURE 6. Variation of moments $\overline{u^n}/(\overline{u^2})^{\frac{1}{2}n}$ along centre line of plane jet. ○, $n = 3$, multiplying factor = 10^{-1}; □, 5, 5; △, 7, 10^3; ●, 4, 1; ■, 6, 50; ▲, 8, 10^4.

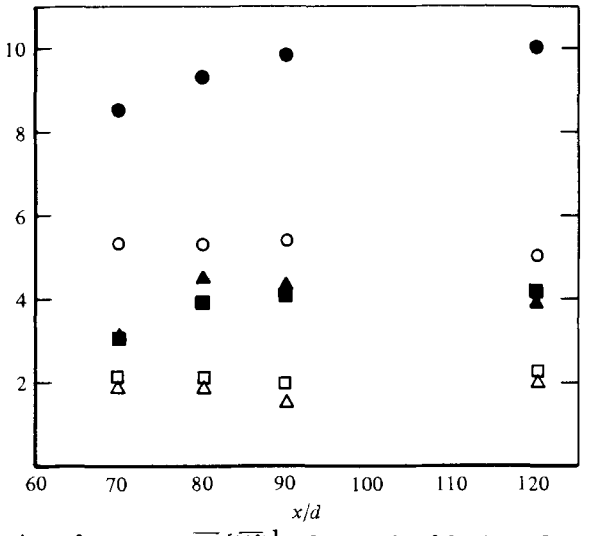

FIGURE 7. Variation of moments $\overline{u^n}/(\overline{u^2})^{\frac{1}{2}n}$ along axis of 2·54 cm diameter jet. ○, $n = 3$, multiplying factor = 10^{-1}; □, 5, 10; △, 7, 10^3; ●, 4, 1; ■, 6, 10^2; ▲, 8, 10^4.

(figure 7) jets indicates that there is little change in the magnitude of normalized moments for $60 \leqslant x/d \leqslant 140$ (plane jet) or $70 \leqslant x/d \leqslant 120$ (circular jet). These ranges for x/d correspond to regions of the flow for which mean-velocity and turbulence-intensity profiles have been measured and found to be approximately self-preserving. While R_λ remains constant on the axis of a circular jet, it increases slowly with x/d on the centre-line of a plane jet. Considerations of self-preservation (Antonia, Satyaprakash & Hussain 1980) indicate that this is the case, and that $R_\lambda \simeq 400$ for the 2·54 cm jet. In the plane jet, R_λ is proportional, as required by self-preservation, to the square root of a local Reynolds number (based on U and L_0, say). However, R_λ increases slightly (Antonia, Satyaprakash & Hussain 1980) with x/d, and this increase appears to be reflected (figure 6) in the increasing trend exhibited by the seventh- and eighth-order moments. Lower-order moments do not seem to reflect the measured

increase in R_λ. No fine-structure measurements have been made, in the present experiment, at small values of x/d. Antonia *et al.* pointed out that, while large values of R_λ, in excess of 1000, are reported in the literature at small x/d, the statistics of the fine-scale velocity field under these conditions probably reflect the effect of initial conditions. To illustrate this point, Keffer, Budny & Kawall (1978)† obtained values of 0·26 and 3·99 for S and F on the axis of a plane jet at $x/d = 12$, where $R_\lambda \simeq 1375$. These values of S and F are clearly much smaller than the values indicated in figure 6.

4.2. *Estimates of* μ

4.2.1. *Moments of* $\dot{u}$. The dependence of Reynolds number R_λ and order n of higher even-order moments $\overline{\dot{u}^{2n}}/(\overline{\dot{u}^2})^n$ (for $n = 2, 3, 4$) is plotted in figure 8 using a method, based on the LN model, suggested by Frenkiel & Klebanoff (1975). These authors neglect the constant A in expression (1) for σ^2, assuming that $r \sim \eta$ and that the Reynolds number is very large.‡ Using the properties of the lognormal distribution, Frenkiel & Klebanoff obtained

$$\frac{\overline{\dot{u}^{2n}}}{(\overline{\dot{u}^2})^n} \sim \left(\frac{L}{\eta}\right)^{\frac{1}{2}\mu n(n-1)} \sim R_\lambda^{\frac{3}{4}\mu n(n-1)}, \tag{9}$$

assuming the isotropic result $L/\eta \sim R_\lambda^{\frac{3}{2}}$. The present data (figure 8) lie slightly above the distribution of Frenkiel & Klebanoff, probably because of the lower filter setting ($f_c = f_K$) used by these authors. Since the local slope of the experimental distribution of figure 8 is, according to (9), proportional to μ, the plot of figure 8 can be thought of as a possible method of determining μ. A straight line of slope corresponding to $\mu = 0{\cdot}2$ represents both the present data and those of Frenkiel & Klebanoff up to a value of $n(n-1)\log_{10} R_\lambda$ of about 20. Frenkiel & Klebanoff have already noted that the decrease in the local slope (or μ) with increasing n or R_λ (note that the plot gives greater weighting to n than to R_λ) cannot be attributed to insufficiently large values of R_λ. The present data have been obtained for values of R_λ (up to about 1000) larger than those considered by Frenkiel & Klebanoff, but for a maximum value ($= 4$) of n that is smaller than their maximum ($= 7$). While they verified that atmospheric data were consistent with their distribution, these data corresponded to $n = 2$ only. According to Tennekes & Wyngaard (1972), the likelihood of obtaining reliable higher-order moments of $\dot{u}$ in the atmosphere is small because of unrealistically large integration times required to achieve statistical stability in the extreme tails of the probability-density function. It has also been suggested (Frenkiel *et al.* 1979) that the decrease of μ with n is universal (at least for a given value of f_c), in the sense that it does not depend on the particular flow. The present data, obtained in different jet flows, provide further support for this suggestion.

The exponent μ has also been estimated from the variance σ^2 (1) of $\ln \epsilon_r$.§ Plots of

† It should be made clear that the measurements of Keffer *et al.* were only made to test a technique for the simultaneous measurement of velocity and temperature in heated turbulent flows.

‡ For the relatively small R_λ range considered by Frenkiel & Klebanoff, the neglect of A is not entirely justifiable. Later in this section A is shown to be of order unity.

§ Assuming Taylor's hypothesis, ϵ_r is obtained by averaging $(\partial u/\partial x)^2$ over a time interval τ (i.e. $r = U\tau$).

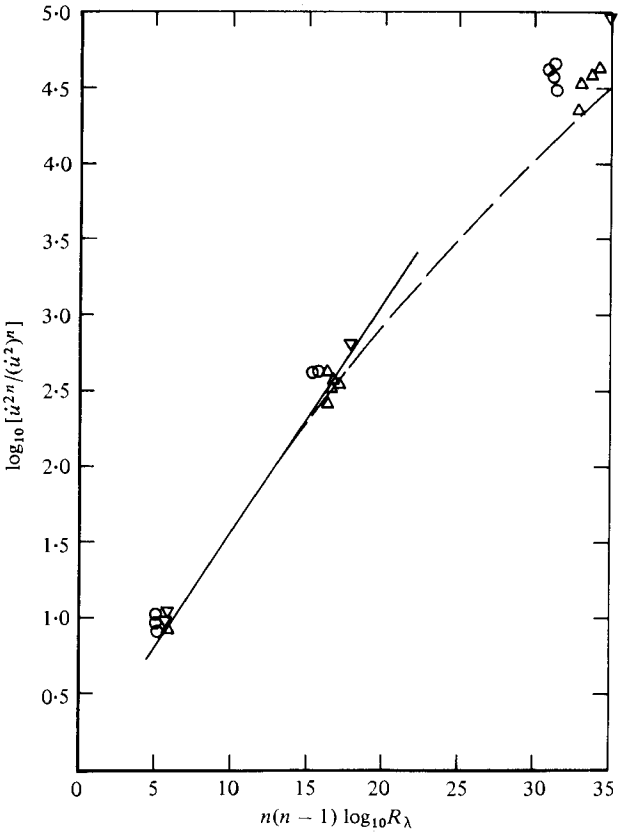

FIGURE 8. Reynolds-number dependence of $\overline{u^{2n}}/(\overline{u^2})^n$ ($n = 2, 3, 4$). Circular jet: ○, $d = 2{\cdot}54$ cm; ▽, 18 cm. Plane jet: △, – – –, Frenkiel & Klebanoff (1975). Solid line has a slope corresponding to $\mu = 0{\cdot}2$ (see (9)).

σ^2 *vs.* $\ln(L/r)$ are shown in figures 9 (circular jet) and 10 (plane jet). The scale L is identified here with the integral length scale derived from the velocity fluctuation u:

$$L = U\int_0^{\tau_0} \frac{\overline{u(t)\,u(t+\tau)}}{\overline{u^2}}\,d\tau,$$

where τ_0 is (arbitrarily) taken as the first zero-crossing point of the autocorrelation. The ratio L/L_0 is approximately constant, equal to about 0·51 along the centre line of the plane jet, and about 0·48 on the axis ($60 < x/d < 160$) of the 2·54 cm circular jet.

The range of $\ln(L/r)$, which is bounded by the vertical bars shown in figures 9 and 10, is the approximate extent of the inertial subrange as deduced from the $r^{\frac{2}{3}}$ behaviour of the second-order velocity structure function (not shown here). The relevance of this choice of subrange to σ^2 is perhaps questionable, since the extent of the inertial subrange may differ significantly for different statistical parameters. It is known (e.g. Monin & Yaglom 1975, pp. 357–358) that inertial subranges of longitudinal, lateral, one-dimensional scalar and three-dimensional spectra are different. In the present paper, the extent of the relatively well-defined two-thirds law is used as an inertial-subrange indicator for σ^2 and high-order correlation and moments of the dissipation. While it is difficult to draw a unique straight line in figures 9 and 10 over

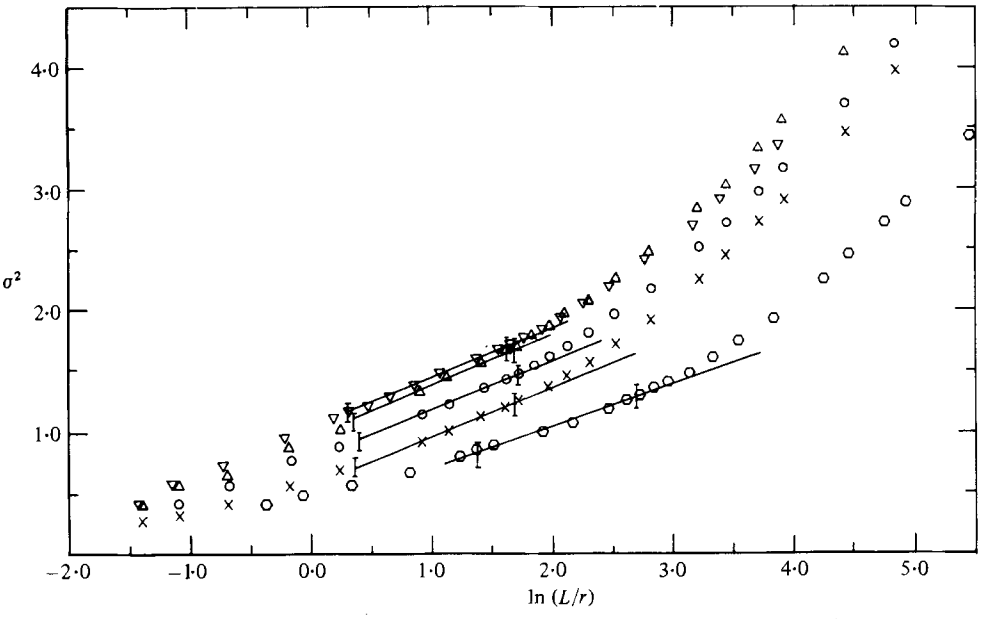

FIGURE 9. Variation of σ^2 with ln r for circular jets (d = 2·54 cm): ×, x/d = 70; ○, 80; △, 90; ▽, 120. Circular jet (d = 18 cm): ○, x/d = 50.

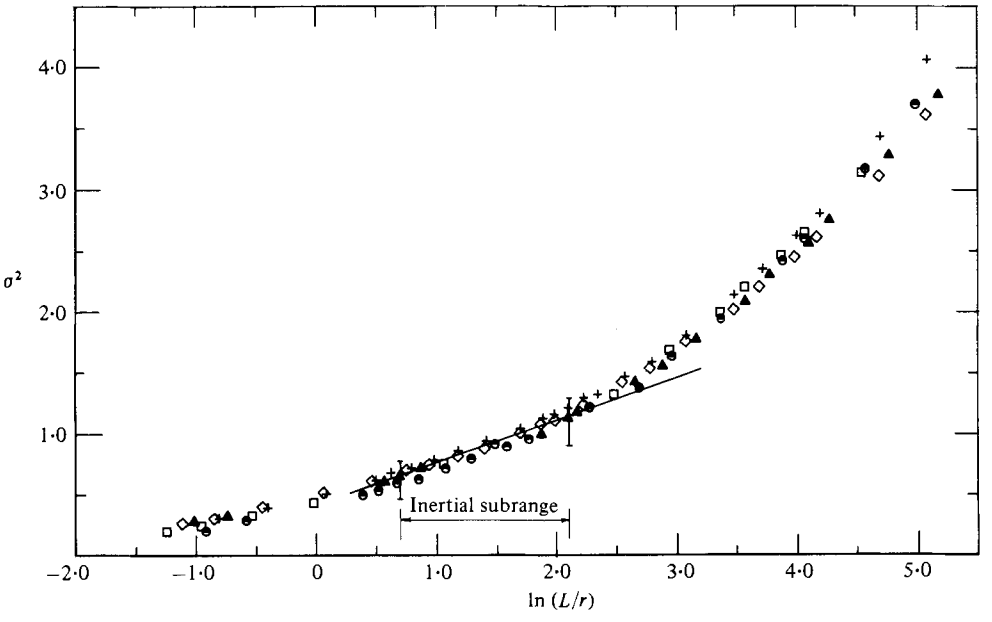

FIGURE 10. Variation of σ^2 with ln r for plane jet: □, x/d = 60; ◓, 80; +, 100, ◇, 120; ▲, 140.

the range of r, the extent of the power law (2) is shown later to overlap the inertial range of r indicated in figures 9 and 10. For the spectral-dissipation data, discussed in § 4.2.3, the extent of the $-\frac{5}{3}$ behaviour in the spectrum of u, or the $+\frac{1}{3}$ behaviour in the $\dot{u}$-spectrum, is used as the inertial-subrange indicator. The straight lines shown in figures 9 and 10 yield $\mu \simeq 0{\cdot}4$ ($\pm$ standard deviation of 0·05) for the 2·54 cm jet, and

$\mu = 0{\cdot}34$ for both the 18 cm jet and the plane jet. These values of μ are approximately twice as large as the value inferred from figure 8. For both the plane jet and the 18 cm circular jet, the additive constant A in (1) is equal to about 0·35, whereas, for the 2·54 cm circular jet, A increases from about 0·6 at $x/d = 70$ to almost 1·0 at $x/d = 120$. There is little difference between values of σ^2 at $x/d = 90$ and $x/d = 120$, suggesting that, in that particular flow, a unique distribution of σ^2 may be reached at large x/d. Distributions of σ^2 in the plane jet ($60 < x/d < 140$) all follow the same distribution. It is difficult to explain the variation with x/d in the circular jet since, as mentioned earlier, approximate self-preservation was established from the experimental range of x/d. It may be tempting to infer, in view of the constancy of A with x for the plane jet, that the dependence on flow macrostructure disappears more quickly in the plane than in the circular jet. However, such an inference seems contrary to the expectation that the far field of the plane jet is perhaps more sensitive to initial conditions (e.g. Gutmark & Wygnanski 1976; Hussain & Clark 1977) than that of a circular jet (Z. D. Husain, private communication). Gibson & Masiello (1972) reported a value for A of $-1{\cdot}2$ in the atmospheric surface layer above the ocean, but in their experiments L was taken as the height (30 m) above the ocean. These authors estimated $\mu \simeq 0{\cdot}5$ from the slope of σ^2 *vs.* $\ln(L/r)$, but the linear region was assumed to cover the approximate range $2 < r/\eta < 100$. The lower bound for r/η is far too small to fall realistically inside the inertial subrange.† Park (1976) has estimated a much wider inertial subrange ($85 < r/\eta < 5600$) for the data of Gibson & Masiello, and he suggested that Gibson & Masiello's σ^2 values are consistent with his own value of $\mu (\simeq 0{\cdot}17)$. While figures 9 and 10 show an expected (asymptotic) approach of σ^2 towards zero at large values of r, no asymptotic approach is observed as $r \to \eta$. Gibson & Masiello (1972) stated that, for $r < \eta$, σ^2 should approach the magnitude of $\ln F$,‡ which does depend on R_λ (e.g. figure 22). The correctness of this statement depends, like the validity of (9), on the assumptions that A is negligible (i.e. $L \gg \eta$) and that the probability density function of $\dot{u}^2$ is lognormal. There does not seem to be unqualified support (e.g. Monin & Yaglom 1975, p. 649) for this last assumption. Departures from lognormality have been observed in probability-density functions of $\dot{u}^2$ at both small values (e.g. Wyngaard & Tennekes 1970) and large values of $\dot{u}^2$ (Saffman (1970) suggests one possibility why a deviation from lognormality might be expected). Gibson & Masiello reported a significant departure from lognormality at small values of $\dot{u}^2$, and attributed it to the fact that the squared derivative is not always proportional to the local dissipation rate. For the present data, the skewness and flatness factors in figure 11 of $\ln \epsilon_r$ or, more correctly,§ $\ln (\partial u/\partial t)_\tau^2$ indicate that the departures from Gaussianity are smaller near $r/\eta \simeq 10$ than over the inertial subrange. However, at $r/\eta \simeq 10$, the magnitude of the skewness deviates significantly from the Gaussian value, while the flatness factor is approximately 3·2. The good collapse observed for the data in figure 10 is only evident at relatively small values of r in figure 11.

It seems worth recalling here that Antonia & Sreenivasan's (1977) measurements

† It has been assumed here that (1) is strictly valid for $\eta \ll r \ll L$, the range for which experimental verification of (1) has been sought.

‡ For $n = 2$, Gibson, Stegen & McConnell (1970) used their atmospheric data to estimate μ from the slope of $\ln F$ *vs.* (L/η). They found $\mu = 0{\cdot}44 \pm 0{\cdot}25$, but their relatively few data, obtained at four heights above the surface of the ocean, exhibited significant scatter.

§ Taylor's hypothesis is assumed, as the averaging was performed over time τ.

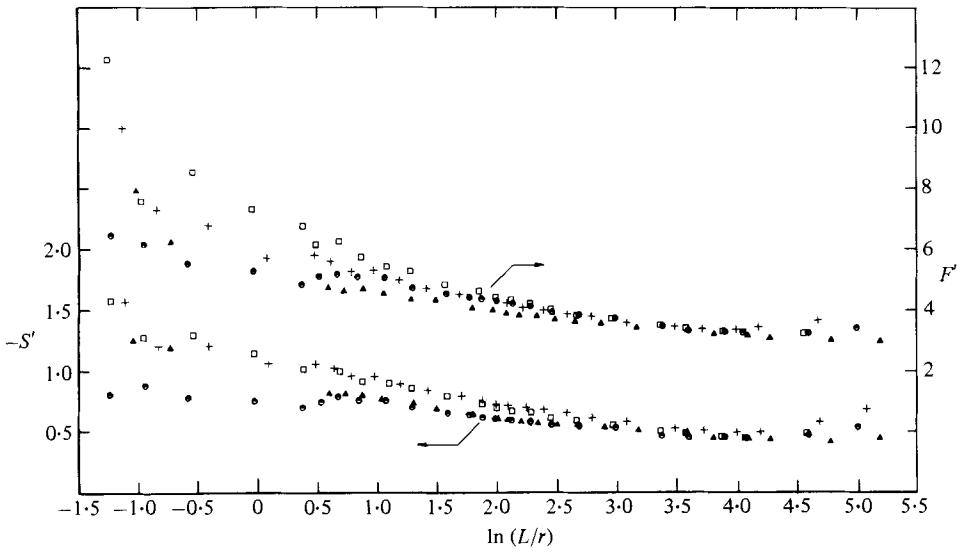

FIGURE 11. Skewness S' and flatness factor F' of $\ln \epsilon_r$ as functions of $\ln r$ for plane jet: □, x/d = 60; ○, 80; +, 100; ▲, 140.

of the temperature dissipation χ (all three components were measured) in a turbulent boundary layer indicated that $p(\chi_r)$ was lognormal over a significant range of r. The variance σ_1^2 of $\ln \chi_r$ plotted in figure 4 of their paper approaches a constant value as $r \to \eta$. The value of μ_θ, exponent analogous to μ, was determined to be 0·35 from the slope of σ_1^2 *vs.* $\ln(L/r)$. This value was only slightly larger than the value of 0·30 inferred from high-order moments of χ_r plotted in a form analogous to that used by Frenkiel & Klebanoff.

4.2.2. *Correlations of* ϵ. Perhaps the most direct way of estimating μ is to measure the spatial correlation of ϵ and to use (2). It is assumed throughout this paper that ϵ is proportional to $(\partial u/\partial x)^2$, its most easily measured component. Gibson & Masiello (1972) have indicated that this assumption may not be reasonable, since contributions to ϵ come largely from cross terms when $(\partial u/\partial x)^2$ is small.† Averaging $(\partial u/\partial x)^2$ over a volume of dimension r does not entirely remove this difficulty. The autocorrelation of ϵ in the present work was obtained by first computing the spectrum of $u^2 - \overline{u^2}$, and then performing an inverse Fourier transform of this spectrum. Autocorrelations of ϵ for both plane and circular (2·54 cm) jets are shown in figure 12 in terms of the coefficient $G_2 \equiv \overline{\epsilon(x)\,\epsilon(x+r)}/\bar{\epsilon}^2$ as a function of L/r. Temporal correlations were computed, and these are interpreted as spatial correlations by using Taylor's hypothesis. The plane jet follows a single distribution, which seems consistent with the collapse onto a unique curve of the σ^2 data (figure 10). For the circular jet, there is a slight increase of G_2 as x/d increases. All the data in figure 12 are consistent with the power-law form of (2). The validity of this power law extends beyond the inertial subrange, whose extent is indicated in the figure. The departure from the power-law behaviour occurs relatively sharply at $L/r \simeq 60$, which corresponds roughly to

† Measurements by Sreenivasan, Antonia & Danh (1977) of χ_r in a turbulent boundary layer indicated that (1) was valid for χ_r over a range of r considerably larger than that exhibited by any individual component of χ_r.

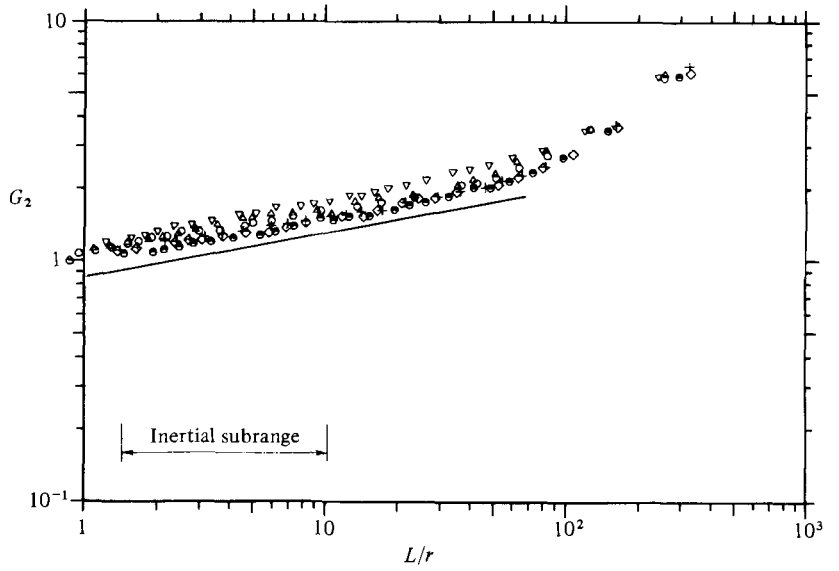

FIGURE 12. Correlation coefficient G_2 as a function of r. Circular jet (d = 2·54 cm): ○, x/d = 80; △, 90; ▽, 120. Plane jet: ◓, x/d = 80; +, 100, ◇, 120.

$r/\eta \simeq 10$ and 7·5 for the plane and circular jets respectively. It should be noted that, as $r \to \eta$, the magnitude of G_2 should approach that of the flatness factor F. At small r, G_2 should therefore reflect the Reynolds-number variation of the flatness factor. This is not evident in figure 12, although the rate of increase of G_2 with L/r is more rapid, at large L/r, for the plane (R_λ = 630) than the circular jet ($R_\lambda \simeq 400$). The slope of the straight line in figure 12 is 0·2; all the data in the figure are consistent with μ = 0·2 ($\pm$ 0·02). The 18 cm jet correlation (Antonia, Phan-Thien & Satyaprakash 1981) also indicate a value of μ of 0·2. The difference in the magnitude of G_2 in the inertial subrange, between the plane jet and the 2·54 cm circular jet, can perhaps be attributed, at least in the context of LN (note that the constant in (2) depends on flow macrostructure), to the difference in flow macrostructure.

It has been noted earlier that predictions by different models of $\overline{\epsilon^m(x)\,\epsilon^m(x+r)}$ should show differences that increase as m increases. Correlations were obtained for m = 1·5 and 2. In the first case, the absolute value of $\dot{u}^3$ was formed before computing the autocorrelation of $|\dot{u}^3|$. The correlations

$$G_3 \equiv \frac{\overline{|\dot{u}^3|(t)\,|\dot{u}^3|(t+\tau)}}{(\overline{\dot{u}^2})^3},$$

$$G_4 \equiv \frac{\overline{\dot{u}^4(t)\,\dot{u}^4(t+\tau)}}{(\overline{\dot{u}^2})^4}$$

are plotted in figures 13 and 14 respectively. The distributions of G_3 and G_4 (the scatter is rather large) appear to be consistent with a power-law behaviour over a range of L/r that coincides approximately with that indicated by the G_2 data. The approximate values of the slopes of the straight lines in figures 13 and 14 are 0·35 and 0·56 respectively. With $\mu \simeq 0{\cdot}20$, LN (equation (3)) predicts exponents of 0·45 and 0·80 for G_3 and G_4, while the β and NS models (equation (4)) yield 0·40 and 0·60

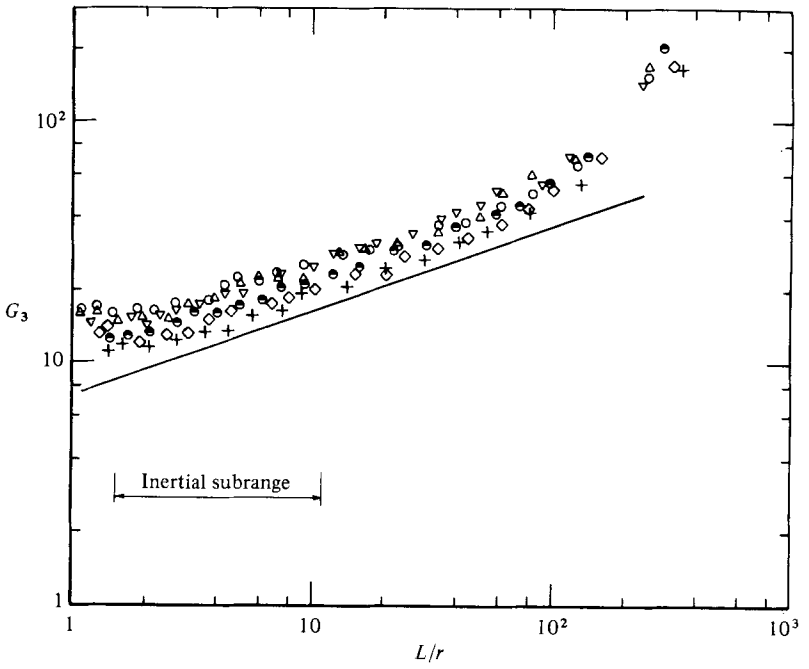

FIGURE 13. Correlation coefficient G_3 as a function of r.
Symbols are same as in figure 12.

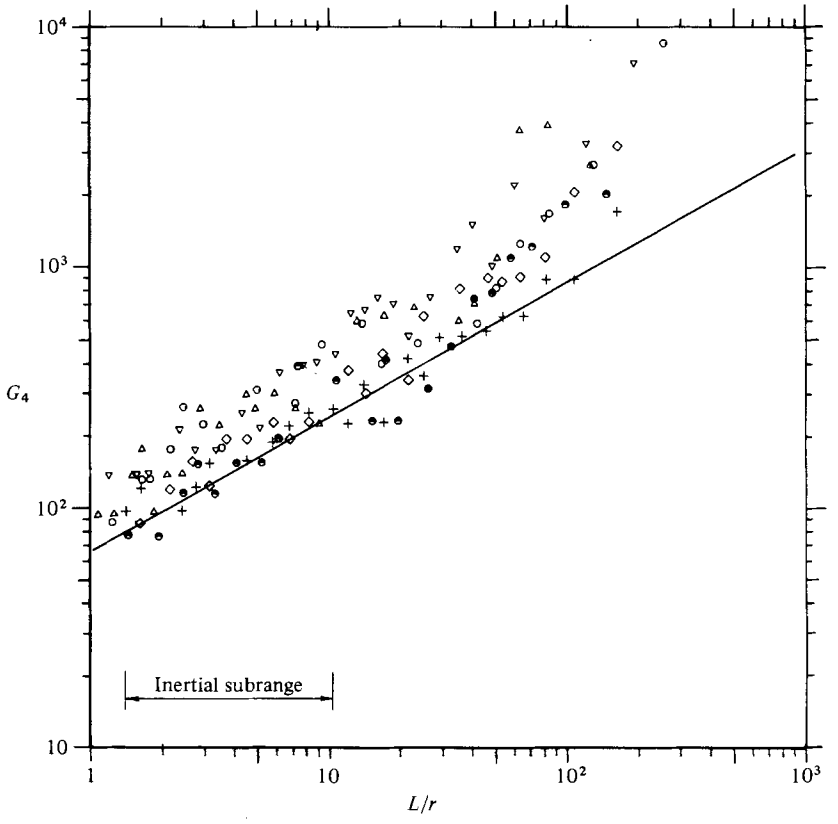

FIGURE 14. Correlation coefficient G_4 as a function of r.
Symbols are same as in figure 12.

respectively. The β and NS models are therefore in closer agreement with the experimental values than are the predictions of LN.

The value $\mu \simeq 0{\cdot}2$ is in reasonable agreement with the value deduced from Gagne & Hopfinger's (1979) measured correlations of ϵ in a fully developed duct flow and in an axisymmetric jet with R_λ in the range 230–500. These authors presented $[\overline{\epsilon^m(x)\,\epsilon^m(x+r)} - (\overline{\epsilon^m})^2]/\overline{\epsilon^{2m}}$ *vs.* r on a log–log plot and inferred from the relatively extensive (almost two decades in r) power-law variation of this ratio (for $m = 1$) that $\mu \simeq 0{\cdot}5$. If their data are replotted in the form $\overline{\epsilon^m(x)\,\epsilon^m(x+r)}/\overline{\epsilon^m}$ *vs.* r, the distributions for $m = 1$ (in their experiment $\overline{\epsilon^2}/\bar{\epsilon}^2 \equiv F \simeq 10$, for $R_\lambda \simeq 310$) exhibit a power-law variation, consistent with $\mu \simeq 0{\cdot}2$. For $m = 2$, their replotted data suggest that the power-law exponent for G_4 is about 0·6, which is in reasonable agreement with the present value.† The empirical relation

$$\overline{\epsilon^m(x)\,\epsilon^m(x+r)} \sim (r/L)^{-\frac{1}{3}\mu(2m+1)}$$

obtained by Gagne & Hopfinger (for $\mu = 0{\cdot}5$) is not in fact relevant to their data; the conclusion that their data are in agreement with the data of Friehe *et al.* and do not support either LN or β-models is also not correct. Their data, like the present data, are in fact in closer agreement with the NS or β-models than with LN.

4.2.3. *Spectrum of* ϵ. Spectral densities corresponding to the correlations of (3) and (4) have been written (m and n are assumed equal here) as

$$\phi_{\epsilon^m}(k_1) \sim k_1^{-1+\mu m^2}, \tag{10}$$

$$\phi_{\epsilon^m}(k_1) \sim k_1^{-1+\mu(2m-1)} \tag{11}$$

for LN and β respectively (see also Novikov 1965). Spectral densities of $\dot{u}^2$, $|\dot{u}^3|$ and $\dot{u}^4$ taken relative to their mean values are shown in figures 15 (circular jet) and 16 (plane jet). The spectral densities in these figures have been normalized such that the areas under the spectra are all equal to unity.‡ With $\mu = 0{\cdot}2$, (10) yields exponents of $-0{\cdot}8$, $-0{\cdot}55$ and $-0{\cdot}2$ for m equal to 1, 1·5 and 2 respectively. The corresponding exponents, using (11), are $-0{\cdot}8$, $-0{\cdot}6$ and $-0{\cdot}4$. The experimental data indicate slopes over the inertial subrange (approximately $0{\cdot}015 < k_1\eta < 0{\cdot}08$, as inferred from the $k_1^{\frac{1}{3}}$ behaviour of $\phi_{\dot{u}}$) of very roughly $-0{\cdot}45$, $-0{\cdot}30$ and $-0{\cdot}10$. These slopes do not agree with the predictions of (10) and (11). They are however in moderate agreement with Friehe *et al.*'s (1971) experimental values of $-0{\cdot}50$, $-0{\cdot}29$, $-0{\cdot}18$. These authors commented that their spectra did not agree with Novikov's (1965) predictions of the subrange slopes, which, for $\mu = 0{\cdot}5$ (the value assumed by Friehe *et al.*), are respectively $-0{\cdot}5$, 0 and $+0{\cdot}5$. The corresponding predictions using LN for $\mu = 0{\cdot}5$ are $-0{\cdot}5$, $+0{\cdot}125$ and $+1$. The latter values indicate an even larger departure from the present measurements for $m = 1{\cdot}5$ and 2. As m increases, the magnitude of the slope of ϕ_{ϵ^m} in the inertial subrange decreases, and a trend towards a plateau is evident as m becomes large. Friehe *et al.* (1971) suggested that this trend is consistent with modelling the $|\dot{u}|^n$ time series by random delta functions for large n.

While different values of μ have been obtained by considering different statistics

† Distributions of G_2 and G_4 obtained from the measurements of Gagne & Hopfinger are shown in figure 17.

‡ Prior to normalization, it was verified that the area under the non-normalized spectrum of $\dot{u}^2 - \overline{\dot{u}^2}$ was equal to $F - 1$ when the area was divided by $\overline{\dot{u}^2}$. Similarly, the non-normalized spectra of $|\dot{u}^3| - \overline{|\dot{u}^3|}$ and $\dot{u}^4 - \overline{\dot{u}^4}$ yielded values of $\overline{\dot{u}^6}/(\overline{\dot{u}^2})^3 - S^2_{|\dot{u}|}$ and $\overline{\dot{u}^8}/(\overline{\dot{u}^2})^4 - F^2$, in good agreement with those obtained directly from $p(\dot{u})$.

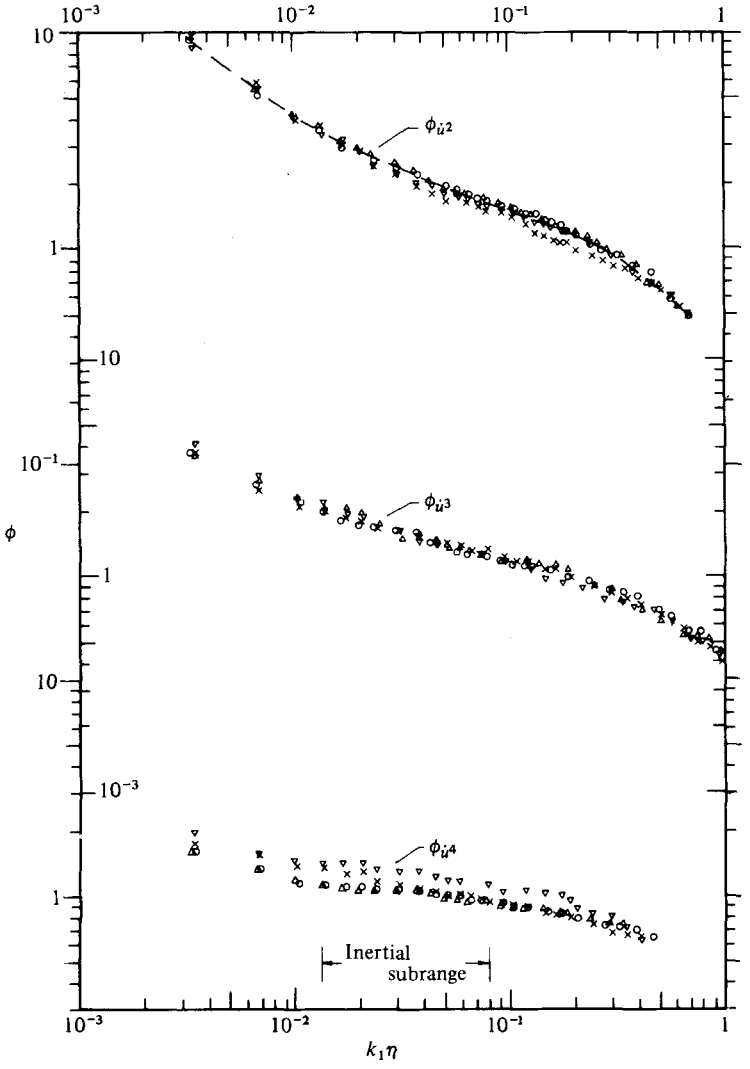

FIGURE 15. Spectra of $\dot{u}^n$ in circular jet (d = 2·54 cm): ×, x/d = 70; ○, 80; △, 90; ▽, 120.

of ϵ obtained from the same data (e.g. Park (1976) obtained $\mu = 0{\cdot}17$ from σ^2 and $\mu \simeq 0{\cdot}4$ from ϕ_ϵ), the discrepancy between the value of μ obtained from the autocorrelation of ϵ and that inferred from the spectrum of ϵ is surprising, since the autocorrelation and spectrum are uniquely related via the Fourier transform. Monin & Yaglom (1975, p. 619) show that the spectrum of ϵ corresponding to the correlation (2) is given as

$$\phi_\epsilon = \frac{1}{\pi}\int_0^\infty [\overline{\epsilon(x)\,\epsilon(x+r)} - \bar{\epsilon}^2]\cos k_1 r\, dr \sim k_1^{-1+\mu},$$

but the limits of integration are not consistent with the range of validity of (2). An explanation for the discrepancy has been provided by Nelkin (1981), who suggested a simple functional form (given below) for the correlation G_2 in the dissipative and inertial regions. The spectrum corresponding to this form was found to fit well

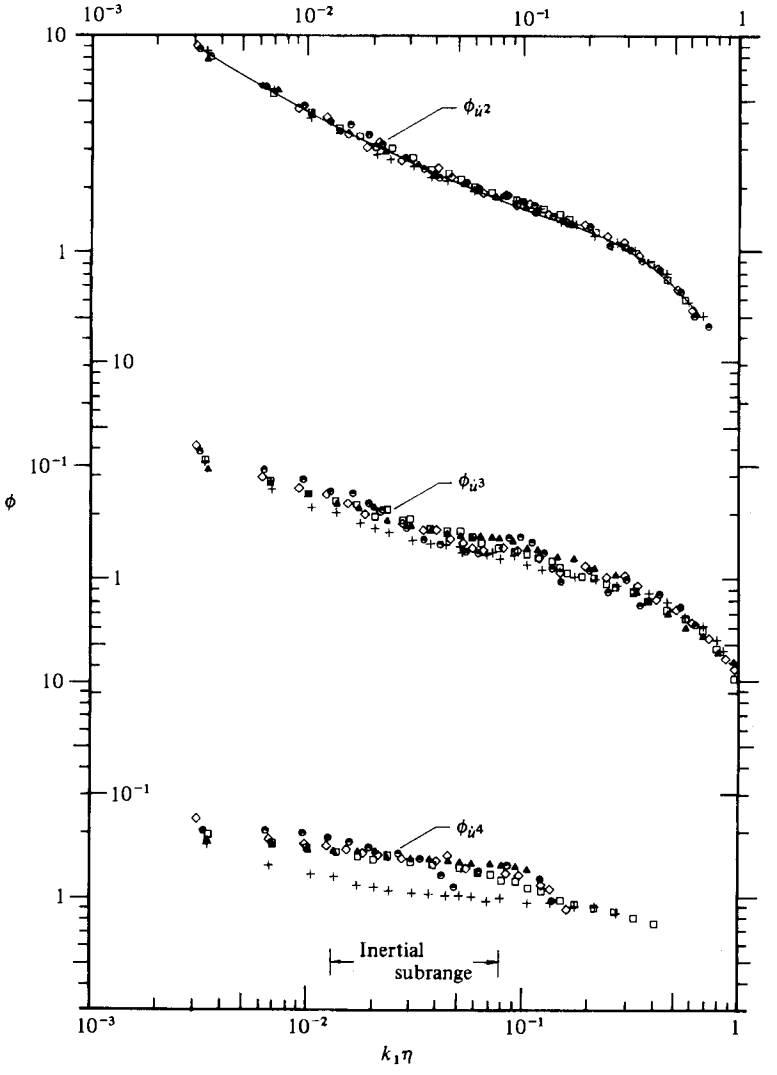

FIGURE 16. Spectra of u^n in plane jet: □, $x/d = 60$; ○, 80; +, 100, ◇, 120; ▲, 140.

Kholmyanskiy's (1972) measurements of ϕ_ϵ in the atmospheric surface layer, and indicated a value of μ of about 0·25, in reasonable agreement with the present correlation estimates. Fitting $k_1^{-1+\mu}$ to Kholmyanskiy's spectrum in the range $0{\cdot}03 < k_1\eta < 0{\cdot}3$ yields a $\mu \simeq 0{\cdot}5$, in reasonable agreement with the value of $\mu \simeq 0{\cdot}55$ inferred from the present ϕ_ϵ spectrum (figure 15). A fit of Kholmyanskiy's spectrum in the range $k_1\eta < 0{\cdot}03$ yields a value of $\mu \simeq 0{\cdot}3$. The different values of μ for different ranges of $k_1\eta$ were already pointed out by Kholmyanskiy. Although an unambiguous selection of the inertial subrange would seem difficult, this difficulty is to a large extent circumvented here by adopting Nelkin's (1981) procedure.

Specifically, Nelkin chose the normalized spectrum ϕ_ϵ to be of the form

$$\phi_\epsilon(k_1\eta) = \frac{e^{-k_1\eta}}{\alpha + \Gamma(\mu)}[\alpha + (k_1\eta)^{\mu-1}], \tag{12}$$

where the parameters α and μ were chosen to fit Kholmyanskiy's (1972) data. The Fourier transform of (12) is

$$G_2 = \alpha\left[\left(\frac{r}{\eta}\right)^2+1\right]^{-1}+\Gamma(\mu)\left[\left(\frac{r}{\eta}\right)^2+1\right]^{-\frac{1}{2}\mu}\cos\left(\mu\arctan\frac{r}{\eta}\right). \tag{13}$$

The shape of G_2 implies the existence of a large peak (the first term on the right of (13)) at small values of r/η, and a long tail (the second term on the right of (13)) proportional to $(r/\eta)^{-\mu}$. The form of G_2 is not inconsistent with that suggested by the physical models, mentioned in § 1, of the fine-structure intermittency, since it reflects the presence of regions of size η in most directions but extended, possibly through interaction with the large-scale motion, in others. As experimental values of G_2 have been obtained, it is more direct to fit G_2 to the correlation data (such data were not available to Nelkin). When $r = 0$, (13) yields

$$G_2(0) \equiv F = \alpha+\Gamma(\mu), \tag{14}$$

thus fixing α. It is clear (figure 17) that (13) with $\alpha = 4{\cdot}75$ and μ taken equal to $0{\cdot}2$ ($\Gamma(0{\cdot}2) = 4{\cdot}59$) is not a good fit to experimental values of G_2 over the inertial subrange (plane-jet data at $x/d = 120$ are shown in figure 17, but it is clear from figure 12 that data from any other station could have been selected; a fit to the $d = 18$ cm circular jet data was considered in Antonia, Phan-Thien & Satyaprakash 1981). A simpler choice for G_2 than that given by (13) is

$$G_2 = \beta[(r/\eta)^2+1]^{-1}+\gamma[(r/\eta)^2+1]^{-\frac{1}{2}\mu}, \tag{15}$$

where β and γ are such that $F = \beta+\gamma$. A fit of (15) to inertial-subrange values of G_2 yields, with μ taken equal to $0{\cdot}2$, $\gamma = 3{\cdot}46$. Equation (15) with $\gamma = 3{\cdot}46$ and $\beta = 5{\cdot}87$ is a better fit, in the range $r/\eta > 10$, to the present data than is (13). The spectral density corresponding to (15) can be shown to be

$$\phi_\epsilon = \frac{1}{\beta+\gamma}\left(\beta e^{-k_1\eta}+\frac{2\gamma}{\pi^{\frac{1}{2}}\Gamma(\frac{1}{2}\mu)}\left(\frac{k_1\eta}{2}\right)^{\frac{1}{2}(\mu-1)}K_{\frac{1}{2}(\mu-1)}(k_1\eta)\right), \tag{16}$$

where K_ν, with $\nu = \frac{1}{2}(\mu-1)$, is the νth-order Bessel function of the second kind. Figure 18 shows the power spectral density estimated using both (12) and (16). Although both equations underestimate the magnitude of the measured spectrum over the inertial subrange (inferred from $+\frac{1}{3}$ behaviour of $\phi^{\dot{u}}$), the slope indicated by (12) for this subrange is only marginally larger than that indicated by (16). The bump in the measured spectrum at $k_1\eta = 0{\cdot}1$ (approximate location of the peak in $\phi_{\dot{u}}$) is underestimated by both (12) and (16). For $k_1\eta > 0{\cdot}8$,† spectral values given by (16) exceed the measured values; the poor agreement between (16) and the measured spectrum at high wavenumbers is not surprising in view of the relatively poor agreement between (15) and measured values of $G_2(r)$ as $r \to 0$.

4.2.4. *Moments of* ϵ_r. The exponent μ can also be obtained from measurements of high-order moments of ϵ_r, since, in general,

$$\overline{\epsilon_r^n} \sim \bar{\epsilon}^n\left(\frac{L}{r}\right)^{\mu n}.$$

† The effect of noise on the spectrum becomes important at $k_1\eta \simeq 1{\cdot}75$.

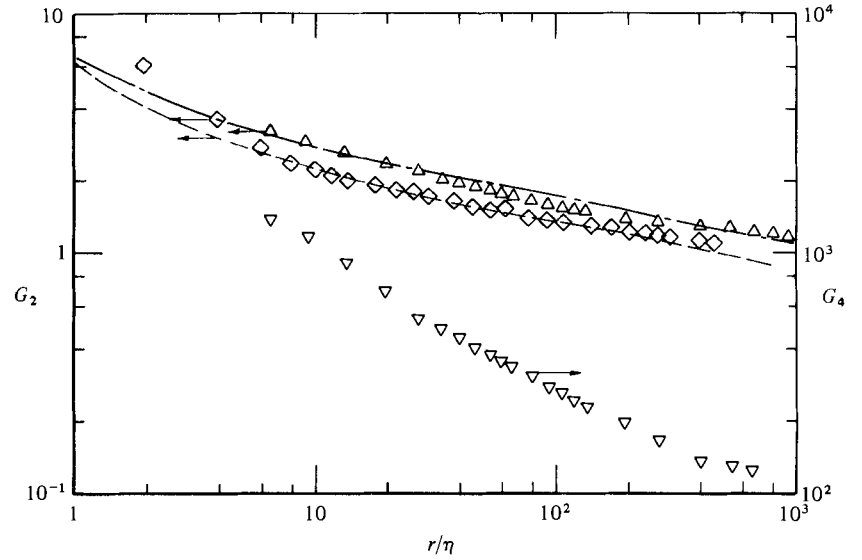

FIGURE 17. Correlation coefficients G_2 and G_4 as functions of r. Plane jet: ◇, 120; – – –, equation (15); — – —, equation (13). Gagne & Hopfinger (1979): △, G_2; ▽, G_4.

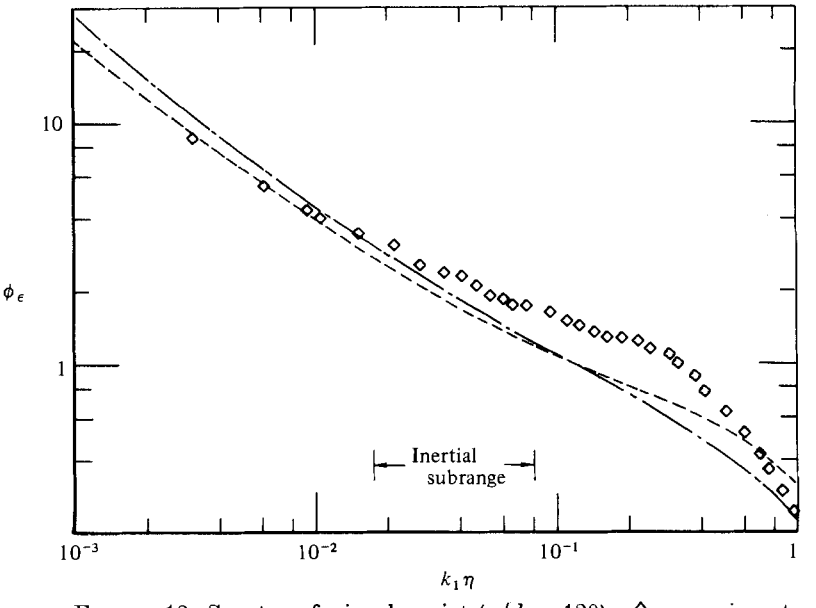

FIGURE 18. Spectra of ϵ in plane jet (x/d = 120): ◇, experiment; – –, equation (16); — – —, equation (12).

For LN, this reduces to (see e.g. Monin & Yaglom 1975, p. 618)

$$\overline{\epsilon_r^n} = \bar{\epsilon}^n \exp\left[\tfrac{1}{2}n(n-1)\,\sigma_r^2\right] = \bar{\epsilon}^n \exp\left[\tfrac{1}{2}n(n-1)\,A\right]\left(\frac{L}{r}\right)^{\frac{1}{2}\mu n(n-1)}, \tag{17a}$$

so that

$$\mu_n = \tfrac{1}{2}\mu n(n-1). \tag{17b}$$

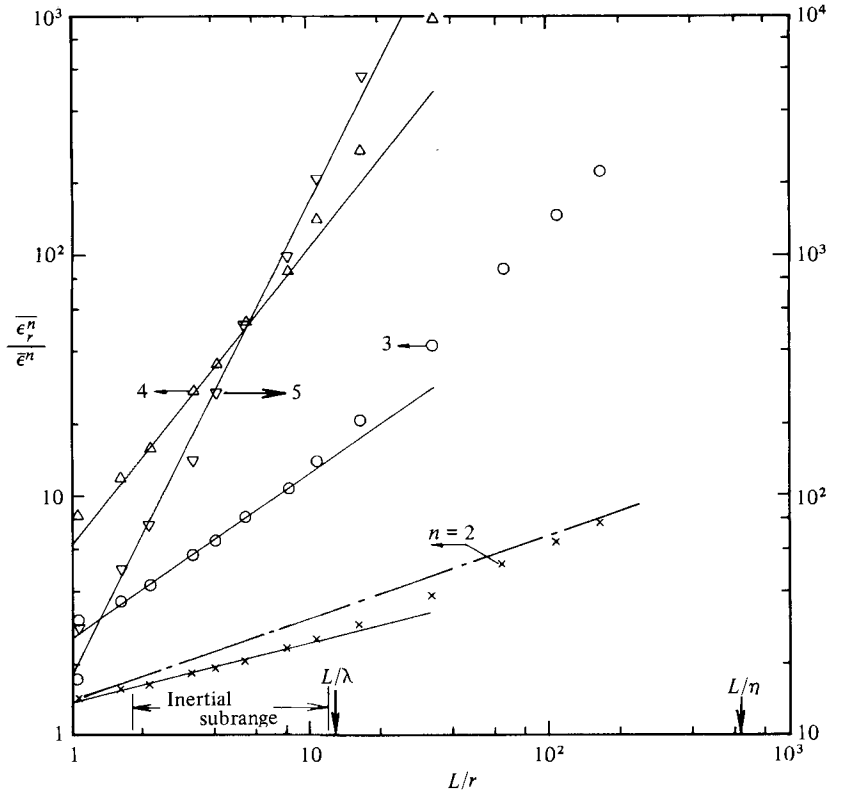

FIGURE 19. Higher-order moments of ϵ_r for plane jet at $x/d = 120$. Straight lines have slopes: $\mu_2 = 0{\cdot}24$; $\mu_3 = 0{\cdot}68$; $\mu_4 = 1{\cdot}20$ and $\mu_5 = 1{\cdot}85$. — - —, equation (17a) with $n = 2$, $A = 0{\cdot}35$, and $\mu = 0{\cdot}34$.

Moments of $\overline{\epsilon_r^n}$, for $n = 2$–5, are shown in figure 19 as functions of L/r. These moments,† obtained in the plane jet at $x/d = 120$, exhibit a good power-law behaviour over a range of L/r that encompasses the inertial subrange. The departure from the power-law behaviour occurs at $L/r \simeq 11$, or very approximately at $r \simeq \lambda$ since, for this particular value of x/d, $L/\lambda \simeq 12$. For small values of r (the value of L/η is shown in figure 19) the ratio $\overline{\epsilon_r^n}/\bar{\epsilon}^n$ should asymptote to the magnitude of the normalized moment $\overline{\dot{u}^{2n}}/(\overline{\dot{u}^2})^n$. The values of μ_n inferred from the straight lines in figure 19 are shown in table 1. For $n = 2$, $\mu_2 \equiv \mu$, and its value, from figure 19, is 0·24. The value of 0·24 shown in table 1 was obtained as an average for different values of x/d; measured values were in the range 0·23–0·25. These values are slightly smaller than the value of 0·28 obtained by Park (1976) and the value of 0·32 reported by Kholmyanskiy (1972), also from atmospheric measurements of $\overline{\epsilon_r^2}$. Kholmyanskiy's values of ϵ_r^n were, however, obtained from a relatively short record ($\simeq 5$ min) and are probably (see Monin & Yaglom 1975, p. 626) not as reliable as those of Park, which were obtained for a 14 min record. The present value of $\mu_2 \equiv \mu$ (table 1) is significantly smaller than the value of $\mu = 0{\cdot}34$, inferred from σ^2 in figure 9. For Park's measurements, μ_2 was larger than the value of 0·17 obtained from σ^2. The difference in the values of μ obtained

† Running values of these moments indicated satisfactory convergence for all values of n considered here. It should be noted that, as in the case of other locally averaged data (e.g. the variance of ϵ_r) presented in the paper, there is no overlap in the computed ranges of τ (or r).

n	Measured,† using $\overline{\epsilon_r^n}$ (present)	Measured, using $\overline{\epsilon_r^n}$ (Kholmyanskiy 1972)	Measured, using $\overline{\epsilon_r^n}$ (Park 1976)	Measured, using breakdown coefficient (Van Atta & Yeh 1973)	Lognormal model $\mu_2 = \mu = 0{\cdot}24$	β-model $\mu_2 = \mu = 0{\cdot}24$	Novikov (1971), based on scale similarity of breakdown coefficient
2	0·24	0·32	0·22	0·15	—	—	0·41
3	0·68	0·95	0·59	0·66	0·72	0·48	1·0
4	1·20	1·65	1·02	1·19	1·44	0·72	1·68
5	1·85	2·34	—‡	—‡	2·40	0·96	2·42

† Values shown here are averages, for different x/d, obtained in plane jet.
‡ Not available.

TABLE 1. Comparison of values of μ_n between experiment and different models

from these two statistics suggests that the lognormal assumption is not satisfied, since we would then expect $\overline{\epsilon_r^2} = \bar{\epsilon}^2 \exp \sigma^2$, a relation that is satisfied by neither the present nor Park's measurements. In figure 19, (17*a*) with $A = 0{\cdot}35$ and $\mu = 0{\cdot}34$, the values obtained from figure 10, overestimates the experimental values over the inertial subrange. Using $\mu_2 = 0{\cdot}24$, the lognormal values of μ_n, (17*b*), are larger (for $n \geqslant 3$) than the measured values, the difference increasing with order n. Park's (1976) measurements of $\overline{\epsilon_r^3}$ and $\overline{\epsilon_r^4}$ yield values of μ_3 and μ_4 in closer agreement with the present values than with those of Kholmyanskiy (1972). The β-model yields values of μ_n given by

$$\mu_n = \mu(n-1). \tag{18}$$

The values of μ_3, μ_4, μ_5 obtained from (18) are significantly smaller than the experimental values (see table 1). LN values of μ_n are in closer agreement with the experiment. This result is in contrast with the previous finding that the exponents in the higher-order correlations of ϵ were more closely represented by the β than the LN model.

4.2.5. *Breakdown coefficients of* ϵ. Also shown in table 1 are the values of μ_n obtained from Novikov's relation

$$\mu_n = n - \log_2(n+1). \tag{19}$$

Equation (19) was obtained by applying scale-similarity arguments to the breakdown coefficient $q_{r,l}$, defined as the ratio of averages over different spatial regions of positive variables associated with small-scale turbulence. Subscripts r and l ($r < l$) denote local averaging of the particular variable chosen over a linear dimension r and l respectively. Novikov considered q to be homogeneous for spatial length scales less than L, and chose a simple form for the probability-density function of $q_{r,l}$. For $n = 2$, (19) gives $\mu_2 = 0{\cdot}41$, which is greater than all other estimates of μ_2 shown in table 1. Novikov's value of μ_2 is certainly greater than the value of 0·15 obtained by Van Atta & Yeh (1973) from direct measurements of the variance of $q_{r,l}$, using experimental data for $\dot{u}$ in an atmospheric boundary layer. Novikov (1971) set out the conditions for scale similarity of $q_{r,l}$ in the interval $\eta \ll r \ll L$. These are that the probability density of $q_{r,l}$ depends only on the ratio l/r, and that adjoint breakdown coefficients $q_{r,r'}$ and $q_{r',l}$ ($\eta \ll r < r' < l \ll L$) are statistically independent. When these conditions are satisfied, the moments of $q_{r,l}$ should exhibit a power-law variation with l/r. Van Atta & Yeh commented that moments of the ratio ϵ_r/ϵ_l did not have the simple power-law character required by scale similarity, and attributed this result to the violation, established by experiment, of the two conditions for scale similarity. Breakdown coefficients of $q_{r,l} (\equiv \dot{u}_r^2/\dot{u}_l^2)$ have been computed for a fixed value ($= 2$) of l/r (segments of length l and r have the same midpoint) and different values of l. Values of μ calculated from the relation

$$\mu = \frac{\sigma_1^2}{\ln(l/r)}, \tag{20}$$

where σ_1^2 is the variance of $\ln q_{r,l}$, are shown in figure 20. As l/η increases, μ approaches a value of about 0·25. The present distribution of μ compares favourably with that, at higher Reynolds number, by Van Atta & Yeh (also for $l/r = 2$). For large values of l/η ($\sim 10^4$), these authors found that μ asymptoted to about 0·15. Kholmyanskiy (1973) found, also using breakdown coefficients, an asymptotic value of μ of about 0·2.

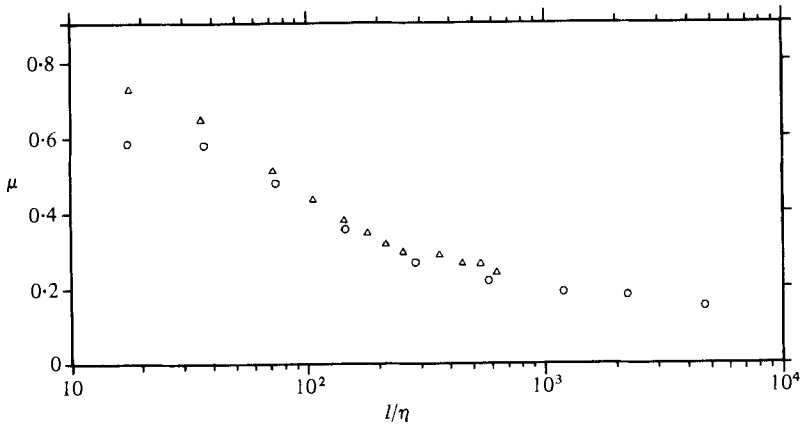

FIGURE 20. Computed values of μ using (20) from breakdown coefficient ϵ_r/ϵ_l. Circular jet (2·54 cm): △, $x/d = 90$; $l/r = 2$. Van Atta & Yeh (1973): ○, $l/r = 2$.

The agreement between their values of μ_3 and μ_4 and those obtained here (and also those of Park) is a little surprising since identification of the present values of $\epsilon_r^n/\epsilon_l^n$ with the corresponding moments of the breakdown coefficient cannot be valid in the limit of large values of l.

5. R_λ variation of S and F

The value of μ inferred from the present correlation measurement of dissipation and from the moments of ϵ_r^n is in reasonable agreement with the value of 0·25 that was found (Van Atta & Antonia 1980) to represent fairly well the variation of S and F over a relatively wide range of R_λ. Van Atta & Antonia examined the influence of fluctuations in ϵ on higher-order structure functions of u for small values of r and on $\overline{\dot{u}^n}$. While methods that have been used (see e.g. Wyngaard & Tennekes 1970; Frenkiel & Klebanoff 1975) to predict the Reynolds-number dependence of high-order moments of $\dot{u}$ have required the value of r to be set explicitly, this requirement was circumvented in the analysis of Van Atta & Antonia. The present data for S and F are shown in figures 21 and 22; other data shown in these figures are essentially contained in figures 1 and 2 of Van Atta & Antonia. The R_λ range covered by the present data is one for which relatively few data are available for S. For example, no measurements of S were made by Kuo & Corrsin (1971) or Gagne & Hopfinger (1979). The present values of S and F are significantly lower than the values (filled-in circles) of Gibson, Stegen & Williams (1970), and are in reasonable agreement with the trend of the predictions of Van Atta & Antonia (straight lines correspond to $\mu = 0{\cdot}25$ and 0·20). It was already pointed out by the latter authors that the R_λ values used for the Gibson *et al.* data are most likely in error. The cut-off frequency used for most of the data (at least for $R_\lambda \gtrsim 100$) was approximately equal to f_K. The present data ($f_c = 1{\cdot}75 f_K$) and those of Gagne & Hopfinger ($f_c = 2f_K$) shown in figure 22 lie generally slightly above other data at corresponding values of R_λ. Before the R_λ trends of S and F can be indicated accurately, the effect of f_c on statistics of $\dot{u}$ for high-R_λ atmospheric data should be ascertained. It is unlikely, however, that the R_λ variations of S and F will differ significantly from those indicated in figures 21 and 22. For $\mu = 0{\cdot}2$, Van Atta

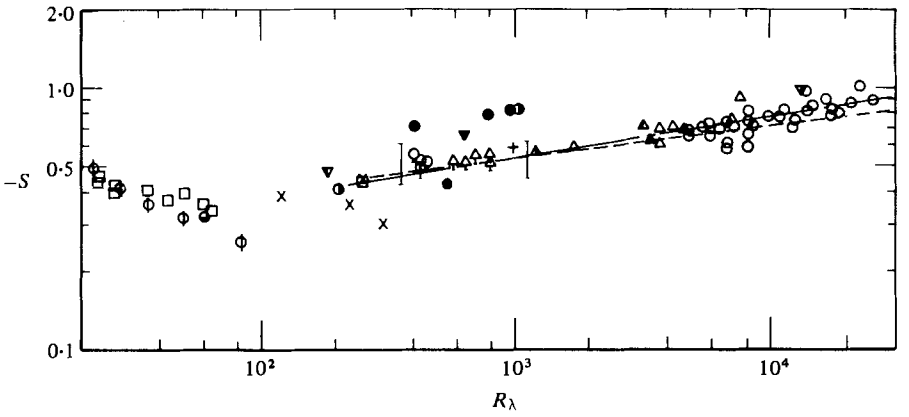

FIGURE 21. Dependence of skewness S on R_λ. Circular jet: ○, d = 2·54 cm; +, 18 cm. Plane jet: △. Vertical bars indicate approximate R_λ range of present data. Van Atta & Antonia (1980): — — —, $|S| \sim R_\lambda^{0.15}$; – – –, $|S| \sim R_\lambda^{0.12}$; □, Batchelor & Townsend (1947, 1949); ϕ, Stewart (1951); ●, Gibson, Stegen & Williams (1970); ○, Wyngaard & Tennekes (1970); △, ▲, McConnell (1976); ◭, Park (1976); ◒, Elena (1977); ◑, Williams & Paulson (1977); ▽, ▼, ▽, Champagne (1978); ×, Comte-Bellot (1963).

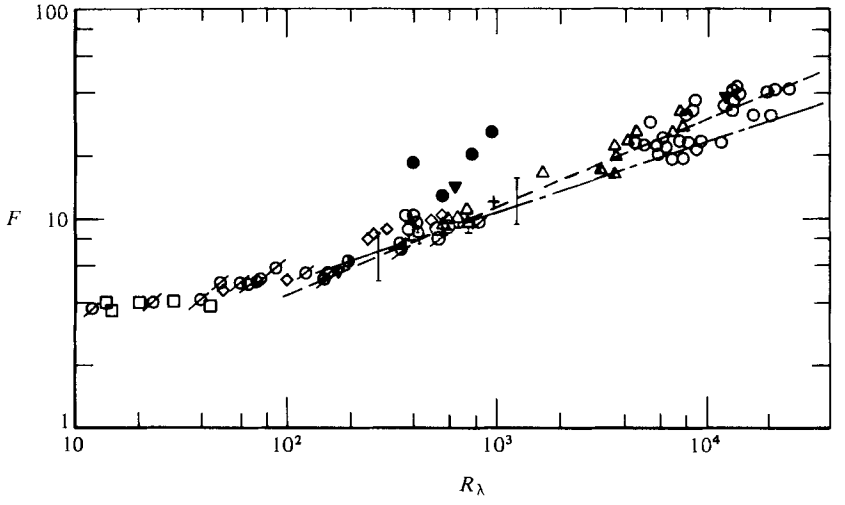

FIGURE 22. Dependence of flatness factor F on R_λ. ◇, Gagne *et al.* (1979); ⌀, Kuo & Corrsin (1971). Other symbols are same as in figure 20. Van Atta & Antonia (1980): – – –, $F \sim R_\lambda^{0.41}$; — — —, $F \sim R_\lambda^{0.32}$.

& Antonia (1980) obtained $-S \sim R_\lambda^{0.12}$ and $F \sim R_\lambda^{0.32}$. It was pointed out that the analysis broke down when $n > (\mu+8)^2/16\mu$, i.e. when $n > 21$ for $\mu = 0{\cdot}2$. This breakdown was tentatively attributed to the basic shortcomings of the LN model. It should be noted that LN models used by Wyngaard & Tennekes (1970) and Frenkiel & Klebanoff (1975) yield $F \sim R_\lambda^{0.31}$ (for $\mu = 0{\cdot}2$) when r is set equal to η. In view of the agreement between the present correlations of ϵ and the predictions of the β-model, it seems appropriate to indicate that the β-model predicts

$$-S \sim R_\lambda^{(3-D)/2(1+D)}, \tag{21}$$

$$F \sim S^2, \tag{22}$$

where $3-D=\mu$, and D is the fractal dimension (see e.g. Mandelbrot 1976). It is clear that (22) does not adequately represent the bulk of experimental data, which suggests (see e.g. Wyngaard & Tennekes 1970; Van Atta & Antonia 1980) that $-S \sim F^{\frac{3}{8}}$ or $F \sim S^{\frac{8}{3}}$. For $\mu \simeq 0{\cdot}2$, (21) yields $-S \sim R_\lambda^{0{\cdot}079}$, which is a slower variation than that suggested by the experimental trend of figure 21.

Van Atta & Antonia (1980) have already suggested that plotting $-S$ *vs.* F is a good way to plot small-scale data. Such a plot involves only information on the fine structure, and circumvents any possible difficulties associated with the use of R_λ. The experimental data obtained in the present investigation are well represented by $-S \sim F^{\frac{3}{8}}$. Cross-plots (Antonia, Chambers & Satyaprakash 1981) of fourth- versus fifth- and of fifth- versus sixth-order moments of the velocity derivative indicated better agreement with the LN than with the β-model.

6. Concluding discussion

A study of the effect of the low-pass filter cut-off f_c on third- and fourth-order moments of $\dot{u}$ has indicated that an appropriate setting for this cut-off is approximately $1{\cdot}75 f_K$. This setting is at variance with the more-frequent setting of f_K used in the literature. While the present recommendation for f_c does not seem to depend on R_λ, it is suggested that the effect of R_λ on f_c should be carefully examined for atmospheric data in order to extend significantly the range of R_λ considered in the present investigation. Record durations required for high-order moments of $\dot{u}$ to converge to within 5 % of their final value were found to be significantly smaller than the total duration of the experimental record. The convergence time is larger for odd- than even-order moments. It is, however, significantly smaller than the integration time estimated using a relation developed by Tennekes & Lumley (1972, p. 212). This latter estimate suffers from increasing inaccuracy as the order of the moment increases in view of experimental inaccuracies in determining high-order moments of $\dot{u}$ and time scales associated with these moments.

The exponent μ has been determined using different statistics of the velocity derivative. The relatively wide range of values of μ reported in the literature seems to indicate that μ is particularly sensitive to the type of statistic that is used. Most investigators have inferred a value of $\mu \simeq 0{\cdot}5$ from the inertial-subrange behaviour of the ϵ-spectrum, but it should be remembered that the precise location of the subrange is not well-known. The use of breakdown coefficients has yielded much lower values of μ. In the present investigation, different estimates of μ are in reasonably good agreement with each other. With the assumption that the dissipation is proportional to $\dot{u}^2$, the dissipation correlation yields $\mu \simeq 0{\cdot}2$, in good agreement with the value of about 0·24 obtained from the inertial-subrange behaviour of the second-order moment of the locally averaged dissipation. The behaviour, at relatively large values of l/η or r/η, of the breakdown coefficient suggests a value of $\mu \simeq 0{\cdot}25$. The behaviour of even moments, up to order 6 of $\dot{u}$, using a method of plotting suggested by Frenkiel & Klebanoff (1975), is consistent with a value of μ of about 0·20. This particular method is based on the assumed lognormality of ϵ_r with $r \equiv \eta$ and the assumed validity of expression (1) for the variance σ^2 when $r = \eta$. The non-universality of μ, as evidenced by the decrease in the slope of $\overline{\dot{u}^{2n}}/(\overline{\dot{u}^2})^n$ in figure 8 as the order n increases, must be viewed in the context of these assumptions. The difference between

the value of μ obtained from the previously mentioned measurements and that inferred (equal to about 0·4) from the variance σ^2 of $\ln \epsilon_r$, where r lies in the inertial subrange, can probably be ascribed to the difficulty in establishing unambiguously the range of validity of (1). Values of μ, deduced from σ^2, reported in the literature range from about 0·17 to 0·5. It was already pointed out in § 4 that different values of μ have been suggested by different authors using the same σ^2 distribution. It is possible that a value of μ of about 0·2 may be consistent with the σ^2 distribution as $r \to \eta$, but such a possibility would require experimental verification. The value of μ inferred from the second-order moment of ϵ_r can only coincide with the value of μ in (1) provided (1) is valid and the lognormal assumption is verified. Present results for the skewness and flatness factors of $\ln \dot{u}_r^2$ and the departure between measured values of $\overline{\epsilon_r^2}$ and those given by (17*a*) suggest that the lognormality of $\dot{u}_r^2$ is, at best, only a rough approximation.

While a value of $\mu \simeq 0{\cdot}5$ is obtained by assuming that the inertial-subrange slope of the spectrum of $\dot{u}^2$ is given by $k_1^{-1+\mu}$, this determination of μ may be in error, since the range of validity of the well-defined power-law behaviour of the autocorrelation of $\dot{u}^2$ is limited nominally to the inertial subrange. This latter information is not reflected in the limits of integration for the Fourier transform of $\dot{u}^2$ from which a $k_1^{-1+\mu}$ behaviour is derived. When the measured autocorrelation of $\dot{u}^2$ is modelled according to a shape suggested by Nelkin (1981), the calculated spectrum of $\dot{u}^2$ is in qualitative agreement with the experimental spectrum, and is consistent with a value of μ equal to 0·2. Values of μ_n, obtained from high-order moments of $\dot{u}_r^2$ are represented more reasonably by predictions from the lognormal than the β-model. In contrast, the β-model is in closer agreement with values of μ_n inferred from high-order correlations of $\dot{u}^2$ than is the lognormal model. These results indicate that the Reynolds-number variation of normalized moments of the velocity derivative is more likely to be approximated by predictions based on the lognormal assumption than by the β-model. This latter model does not predict satisfactorily the variation of the experimental skewness and flatness factors of the velocity derivative. It appears, however, that spatial correlations of the dissipation field or other quantities associated with the fine structure of turbulence will be better approximated by the NS or β-models than by the LN model. It also seems that physical models, which are consistent with an ϵ-autocorrelation of the form given by G_2, are likely to help unravel the spatial geometry of the fine structure.

R.A.A. acknowledges the support of the Australian Research Grants Committee. A.K.M.F.H. acknowledges support by the U.S. National Science Foundation under Grant ENG75-15226. The authors would like to thank one of the referees for detailed comments on the manuscript. The comments by Dr E. Hopfinger are also gratefully acknowledged.

REFERENCES

ANTONIA, R. A., CHAMBERS, A. J. & SATYAPRAKASH, B. R. 1981 *Univ. Newcastle, N.S.W., Dept. Mech. Engng Rep.* TN-FM 52.

ANTONIA, R. A., PHAN-THIEN, N. & CHAMBERS, A. J. 1980 *J. Fluid Mech.* **100**, 193.

ANTONIA, R. A., PHAN-THIEN, N. & SATYAPRAKASH, B. R. 1981 *Phys. Fluids* **24**, 554.

ANTONIA, R. A., SATYAPRAKASH, B. R. & HUSSAIN, A. K. M. F. 1980 *Phys. Fluids* **23**, 695.

ANTONIA, R. A. & SREENIVASAN, K. R. 1977 *Phys. Fluids* **20**, 1800.

ANTONIA, R. A. & VAN ATTA, C. W. 1978 *Phys. Fluids* **21**, 1096.

BATCHELOR, G. K. & TOWNSEND, A. A. 1947 *Proc. R. Soc. Lond.* A **190**, 534.

BATCHELOR, G. K. & TOWNSEND, A. A. 1949 *Proc. R. Soc. Lond.* A **199**, 238.

BRADSHAW, P. 1971 *An Introduction to Turbulence and its Measurement.* Pergamon.

CHAMPAGNE, F. H. 1978 *J. Fluid Mech.* **86**, 67.

CHAMPAGNE, F. H., PAO, Y. H. & WYGNANSKI, I. J. 1976 *J. Fluid Mech.* **74**, 209.

CHAMPAGNE, F. H., SLEICHER, C. A. & WEHRMANN, O. H. 1967 *J. Fluid Mech.* **28**, 153.

CHOCK, D. P. 1978 *Boundary-Layer Met.* **14**, 397.

COMTE-BELLOT, G. 1963 Ph.D. thesis, University of Grenoble (English transl. (1969) by P. Bradshaw, ARC 31609, FM 41202).

CORRSIN, S. 1962 *Phys. Fluids* **5**, 1301.

ELENA, M. 1977 *Int. J. Heat Mass Transfer* **20**, 935.

FRENKIEL, F. M. & KLEBANOFF, P. S. 1975 *Boundary-Layer Met.* **8**, 173.

FRENKIEL, F. M., KLEBANOFF, P. S. & HUANG, T. 1979 *Phys. Fluids* **22**, 1606.

FRIEHE, C. A., VAN ATTA, C. W. & GIBSON, C. H. 1971 In *Proc. AGARD Special Meeting on Turbulent Shear Flows, London*, 18.1.

FRISCH, U., SULEM, P.-L. & NELKIN, M. 1978 *J. Fluid Mech.* **87**, 719.

GAGNE, Y. & HOPFINGER, E. J. 1979 In *Proc. 2nd Int. Turbulent Shear Flow Conf., Imperial Coll., London*, 11.7.

GAGNE, Y., HOPFINGER, E. J. & MARECHAL, J. 1979 In *Proc. Dynamic Flow Conf.*, 1978, *Marseille and Baltimore* (ed. L. S. G. Kovasznay, A. Favre, P. Buchhave, L. Fulachier & B. W. Hansen).

GIBSON, C. H. & MASIELLO, P. J. 1972 In *Statistical Models and Turbulence* (ed. M. Rosenblatt & C. W. Van Atta), Lecture Notes in Physics, vol. 12, p. 427. Springer.

GIBSON, C. H., STEGEN, G. R. & MCCONNELL, S. 1970 *Phys. Fluids* **13**, 2448.

GIBSON, C. H., STEGEN, G. R. & WILLIAMS, R. B. 1970 *J. Fluid Mech.* **41**, 153.

GURVICH, A. S. & YAGLOM, A. M. 1967 *Phys. Fluids* **10**, S59.

GUTMARK, E. & WYGNANSKI, I. 1976 *J. Fluid Mech.* **73**, 465.

HESKESTAD, G. 1965 *Trans. A.S.M.E.* E, *J. Appl. Mech.* **87**, 735.

HUSAIN, Z. D. & HUSSAIN, A. K. M. F. 1979 *A.I.A.A. J.* **17**, 48.

HUSSAIN, A. K. M. F. 1980 *Lecture Notes in Physics*, vol. 136, p. 252. Springer.

HUSSAIN, A. K. M. F. & CLARK, A. R. 1977 *Phys. Fluids* **20**, 1416.

HUSSAIN, A. K. M. F. & RAMJEE, V. 1976 *J. Fluids Engng* **98**, 58.

HUSSAIN, A. K. M. F. & ZEDAN, M. F. 1978 *Phys. Fluids* **21**, 1100.

KEFFER, J. F., BUDNY, R. S. & KAWALL, J. G. 1978 *Rev. Sci. Instrum.* **49**, 1343.

KHOLMYANSKIY, M. Z. 1972 *Izv. Atmos. & Oceanic Phys.* **8**, 818.

KHOLMYANSKIY, M. Z. 1973 *Izv. Atmos. & Oceanic Phys.* **9**, 453.

KOLMOGOROV, A. N. 1941 *Dokl. Akad. Nauk SSSR* **30**, 301.

KOLMOGOROV, A. N. 1962 *J. Fluid Mech.* **13**, 82.

KRAICHNAN, R. H. 1974 *J. Fluid Mech.* **62**, 305.

KUO, A. Y. & CORRSIN, S. 1971 *J. Fluid Mech.* **50**, 285.

LANDAU, L. D. & LIFSCHITZ, E. 1959 *Fluid Mechanics.* Addison-Wesley.

LUMLEY, J. L. 1965 *Phys. Fluids* **8**, 1056.

LUMLEY, J. L. 1970 *Stochastic Tools in Turbulence*, p. 72. Academic.

MCCONNELL, S. O. 1976 Ph.D. thesis, Univ. California, San Diego.

MANDELBROT, B. 1974 *J. Fluid Mech.* **62**, 331.

MANDELBROT, B. 1976 In *Lecture Notes in Mathematics: Turbulence and Navier Stokes Equation.* Orsay.

MONIN, A. S. & YAGLOM, A. M. 1975 *Statistical Fluid Mechanics: Mechanics of Turbulence*, vol. 2. M.I.T. Press.

NELKIN, M. 1981 *Phys. Fluids* **24**, 556.

NELKIN, M. & BELL, T. L. 1978 *Phys. Rev.* A **17**, 363.

NOVIKOV, E. A. 1965 *Izv. Atmos. & Oceanic Phys.* **1**, 788.

NOVIKOV, E. A. 1971 *Prikl. Math. Mech.* **35**, 266.

NOVIKOV, E. A. & STEWART, R. W. 1964 *Izv. Akad. Nauk Ser. Geophys.* **3**, 408.

OBUKHOV, A. M. 1941 *Izv. Nauk SSSR, Ser. Geogr.: Geofiz.* **5**, 453.

OBUKHOV, A. M. 1962 *J. Fluid Mech.* **13**, 77.

PAO, Y. H. 1965 *Phys. Fluids* **8**, 1063.

PARK, J. T. 1976 Ph.D. thesis, Univ. California, San Diego.

SAFFMAN, P. G. 1970 *Phys. Fluids* **13**, 2193.

SAFFMAN, P. G. 1978 In *Structure and Mechanics of Turbulence II* (ed. H. Fiedler), Lecture Notes in Physics, vol. 76, p. 273. Springer.

SCHEDVIN, J., STEGEN, G. R. & GIBSON, C. G. 1974 *J. Fluid Mech.* **65**, 561.

SREENIVASAN, K. R., ANTONIA, R. A. & DANH, H. Q. 1977 *Phys. Fluids* **20**, 1238.

SREENIVASAN, K. R., CHAMBERS, A. J. & ANTONIA, R. A. 1978 *Boundary-Layer Met.* **14**, 341.

STEWART, R. W. 1951 *Proc. Camb. Phil. Soc.* **47**, 146.

TENNEKES, H. 1968 *Phys. Fluids* **11**, 669.

TENNEKES, H. & LUMLEY, J. L. 1972 *A First Course in Turbulence*. M.I.T. Press.

TENNEKES, H. & WYNGAARD, J. C. 1972 *J. Fluid Mech.* **55**, 93.

TOWNSEND, A. A. 1951 *Proc. R. Soc. Lond.* A **208**, 534.

VAN ATTA, C. W. & ANTONIA, R. A. 1980 *Phys. Fluids* **23**, 252.

VAN ATTA, C. W. & YEH, T. T. 1973 *J. Fluid Mech.* **59**, 537.

WILLIAMS, R. M. & PAULSON, C. A. 1977 *J. Fluid Mech.* **83**, 547.

WYNGAARD, J. C. 1968 *J. Sci. Instrum.* **1**, 1105.

WYNGAARD, J. C. 1973 In *Workshop on Micrometeorology* (ed. D. A. Haugen), p. 101. Am. Met. Soc.

WYNGAARD, J. C. & PAO, Y. H. 1972 In *Statistical Models and Turbulence* (ed. M. Rosenblath & C. Van Atta). Lecture Notes in Physics, vol. 12, p. 384. Springer.

WYNGAARD, J. C. & TENNEKES, H. 1970 *Phys. Fluids* **13**, 1962.

YAGLOM, A. M. 1966 *Sov. Phys. Dokl.* **11**, 26.